GEOLOGICA CARPATHICA, DECEMBER 2015, 66, 6, 515–534 doi: 10.1515/geoca-2015-0042

Source areas of the Grybów sub-basin: micropaleontological, mineralogical and geochemical provenance analysis (Outer Western Carpathians, Poland)

MARTA OSZCZYPKO-CLOWES, PATRYCJA WÓJCIK-TABOL and MATEUSZ PŁOSZAJ

Institute of Geological Sciences, Jagiellonian University, Oleandry 2a, PL 30-063, Kraków, Poland;
m.oszczypko-clowes@uj.edu.pl; p.wojcik-tabol@uj.edu.pl;

(Manuscript received January 10, 2015; accepted in revised form August 22, 2015)

Abstract: The Grybów Unit occurring in the Ropa tectonic window was the subject of micropaleontological and geochemical investigation. Studies, based on calcareous nannofossils, proved that the level of reworked microfossil is not higher than 22 % and it varies between two sections. Quantitative analyses of the reworked assemblages confirmed the domination of Cretaceous and Middle Eocene species. The Sub-Grybów Beds, Grybów Marl Formation and Krosno Beds were assigned to the Late Oligocene and represent the terminal flysch facies. Detrital material accumulated in the Oligocene sediments originated from the Marmarosh Massif, which is the eastern prolongation of the Fore-Magura Ridge. The microscopically obtained petrological features agree with the chemical composition of the samples. Mica flakes, rounded grains of glauconite, heavy mineral assemblage, including abraded grains of zircon, rutile and tourmaline as well as charred pieces of plant tissues are reworked components. Enrichment in zircon and rutile is confirmed geochemically by positive correlation between Zr and SiO_2. Zr addition is illustrated on $10\times Al_2O_3$–Zr–$200\times TiO_2$ and Zr/Sc vs. Th/Sc diagrams. Interpretation of the A–CN–K diagram and variety of CIA and CPA values indicate that the source rocks were intensely weathered granite-type rocks.

Key words: Grybów Unit, Ropa tectonic window, Oligocene, calcareous nannofossils, mineral composition, geochemistry, recycling.

Introduction

In the Polish sector of the Magura Nappe eleven tectonic windows of the Grybów Unit have been recognized (Fig. 1; see also Książkiewicz 1972). This unit is composed predominantly of Upper Eocene–Oligocene deposits (Sikora 1960; Kozikowski 1965; Oszczypko-Clowes & Oszczypko 2004; Oszczypko-Clowes & Ślączka 2006; Oszczypko-Clowes 2008; Oszczypko & Oszczypko-Clowes 2011). The Grybów Unit (Świdziski 1963), known also as the Ropa-Pisarzowa

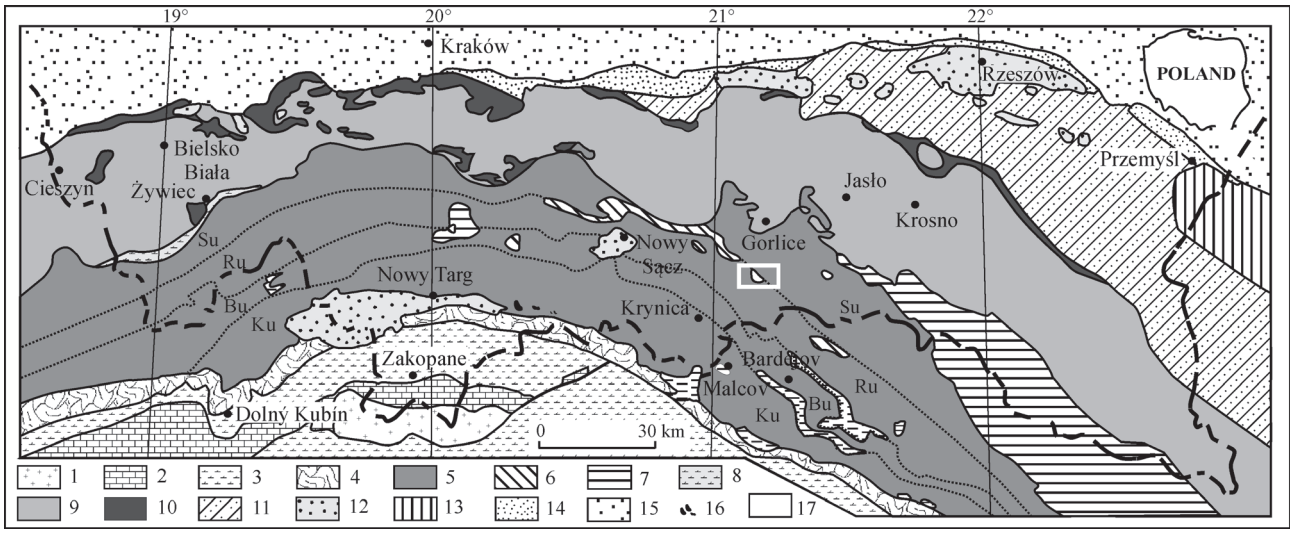

Fig. 1. Tectonic map of the Northern Carpathians (compiled by Oszczypko-Clowes 2001). **1** — crystalline core of the Tatra Mts, **2** — High Tatra and sub-Tatra units, **3** — Podhale flysch, **4** — Pieniny Klippen Belt, **5** — Magura Nappe, **6** — Grybów Nappe, **7** — Dukla Nappe, **8** — Fore-Magura thrust-sheet, **9** — Silesian Unit, **10** — Sub-Silesian Unit, **11** — Skole Unit, **12** — Miocene deposits upon the Carpathian, **13** — Stebnik (Sambir) Unit, **14** — Zgłobice Unit, **15** — Miocene of the Carpathian Foredeep, **16** — andesite, **17** — studied area. **Su** — Siary, **Ru** — Rača, **Bu** — Bystrica, **Ku** — Krynica subunits.

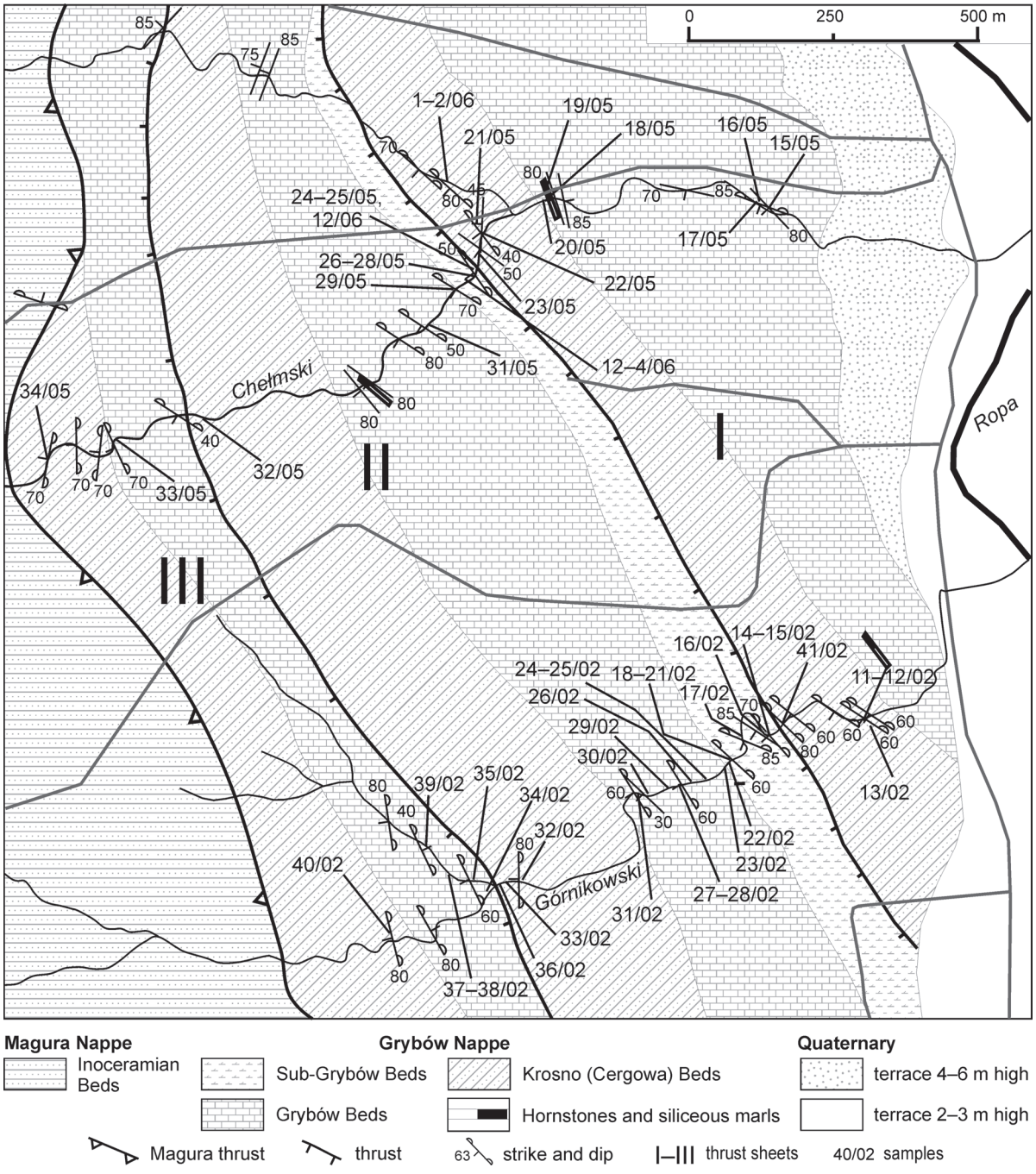

Fig. 2. Geological map of the Ropa tectonic window (Sikora 1960; Oszczypko-Clowes 2008, changed).

Unit (Kozikowski 1956), belongs to the Fore Magura Group of units, which were formed just before the latest Oligocene thrusting of the Magura Nappe onto the Fore-Magura sedimentary area.

The aim of this study was to determine the provenance of the clastic material, reconstruction of source rock lithology as well as interpretation of the source area based on reworked microfossils.

The provenance of the siliciclastic facies sediments of the Outer Carpathians has been studied during the last decades (see Wójcik-Tabol & Ślączka 2013 with references therein). Recycling processes often involve the cannibalistic turnover of the sedimentary mass (McLennan et al. 1993; Veizer & MacKenzie 2003), thus producing shales with moderate geochemical maturity. Heavy minerals, such as zircon and rutile are considered to be the most resistant to degradation during sedimentary reworking. Zircon is a carrier mineral of Zr and Hf. Rutile could have been attributed to TiO_2 contents if titanium had not been easily incorporated by phyllosilicates. A ternary plot of $10\times Al_2O_3$–Zr–$200\times TiO_2$ (Garcia et al. 1991) shows an accumulation of Zr or TiO_2 due to detritus recycling. The Zr/Sc vs. Th/Sc diagram (McLennan et al.

1993) is used to illustrate an addition of reworked material represented by zircon. The CIA index and A–CN–K plot show of source rocks weathering. They also suggest the recycling influence on distribution of major oxides.

Geological framework and studied sections

The oldest sediments of the Grybów Unit belong to the Jaworzynka Beds (Senonian–Paleocene) described from the Mszana Dolna tectonic window (see Oszczypko-Clowes & Oszczypko 2004). The Jaworzynka Beds comprise packets of thick-bedded, biotitic sandstones and conglomerates overlain by thin-bedded, dark, non-calcareous flysch.

The Eocene is represented by the Hieroglyphic Beds (Sikora 1960, 1970) or the Klęczany Beds (Kozikowski 1956) developed as green, grey and black shales, with intercalations of fine- to medium-grained glauconitic sandstones. Towards the top they pass into the Upper Eocene greenish marl with abundant *Globigerina c*orresponding to the Sub-Menilite Globigerina Marls that comprise a key-horizon for all units of the Outer Carpathians (Olszewska 1983; Oszczypko (Clowes) 1996; Leszczyński 1997).

The Oligocene strata are developed as a series of 150 m thick green, grey and black marls, and marly shales with intercalations of thin- to medium-bedded, micaceous and glauconitic sandstones of the Sub-Grybów Beds (S-GB; Kozikowski 1956).

The Sub-Grybów Beds are followed by the Grybów Marl Formation (GMF — after Oszczypko-Clowes & Ślączka 2006) known earlier as Grybów shales (Uhlig 1888; Sikora 1960) or Grybów Beds (Kozikowski 1956). Series up to 200 m thick contain black and brownish-black, platy splitting marls, rarely interbedded by grey marls and sandstones. Thick lenses of ferruginous dolomites occur within the upper part of this series. The highest part of the Grybów Marl Formation contains intercalations of siliceous marls with cherts.

Further up the section there is 400 m thick series of grey, calcareous shales and micaceous sandstones regarded as the Krosno Beds (Kozikowski 1956; Oszczypko-Clowes 2008; Oszczypko & Oszczypko-Clowes 2011). However, Ślączka (1971) and Koráb & Ďurkovič (1978) proposed that they may represent the Cergowa Beds, typical for the Dukla Unit.

The biostratigraphical framework was developed by Kozikowski & Jednorowska (1957), Blaicher (1958), Olszewska (1981), Smagowicz (in Burtan et al. 1992), Smagowicz (in Cieszkowski 1992), Oszczypko-Clowes & Oszczypko (2004), Gedl (2005), Oszczypko-Clowes & Ślączka (2006), Oszczypko-Clowes (2008), Oszczypko & Oszczypko-Clowes (2011).

The Ropa tectonic window is located ca. 15 km SW from Gorlice. Research interest was focused on two sections along the Górnikowski and Chełmski creeks, left bank tributaries of the Ropa River (Figs.1 and 2).

Both sections were described by Kozikowski (1956), Sikora (1960, 1970), Ślączka (1973) and Oszczypko-Clowes (2008). Sikora (1960, 1970) distinguished four thrust-sheets outcropping the Hieroglyphic Beds, Sub-Menilite Globigerina Marls, Sub-Grybów Beds, Grybów Beds and Krosno Beds (Fig. 3). During the latest field works these lithostratigraphic divisions were recognized with the exception of the Hierolyphic Beds and Globigerina Marls (Oszczypko-Clowes 2008). Kozikowski (1956) and Kozikowski & Jednorowska (1957) proposed that the oldest strata of the Ropa tectonic window are represented by the Sub-Grybów Beds. Oszczypko-Clowes (2008) confirmed it. The S-GB exposed in the Górnikowski and Chełmski brooks at the top of thrust-sheet II are developed as brown marly mudstones with intercalations of green and black non-calcareous shales. Calcareous turbidites with Tbc and Tabc Bouma intervals are more typical for the upper part of the Sub-Grybów Beds (Fig. 3). The bluish, micaceous, fine- to medium-grained, thick-bedded sandstones (up to 1.2 m) intercalate the grey, green and black marly shales.

The Grybów Marl Formation can be seen in all thrust-sheets (Figs. 2 and 3). The formation is composed of black, hard marls alternated with dark grey soft marls and fine-grained sandstones with Tab and Tbc Bouma intervals. The upper part of the formation contains ferruginous dolomite layers. In the highest part of the Grybów Marl Formation silicified marls with layers of chert a few cm thick appear (Fig. 3).

The Jasło Limestone layer, exposed in the Górnikowski brook ends the Grybów Marl Formation and forms the border with the overlying Krosno Beds (Kozikowski 1956; Sikora 1960, 1970; Oszczypko-Clowes 2008) or Cergowa Beds (Ślączka 1971; Koráb & Ďurkovič 1978).

Going up the sections the frequency of sandstone decreases and marly pelites dominate. The pelites are represented by dark grey marly shales with intercalations of thin-bedded, cross-laminated calcareous sandstones (Fig. 3). According to Oszczypko-Clowes (2008) it is better to correlate these beds with the Krosno shale lithofacies than with the Cergowa Beds, which are dominated by thick-bedded sandstones (cf. Ślączka 1971).

Samples and methods

All the samples were collected during the field work of the first author. For the purpose of this work only selected samples from the Górnikowski and Chełmski brooks were used.

For the purpose of micropaleontological studies, all samples were prepared using standard smear slide techniques for the light microscope (LM) and then analysed with a Nikon-Eclipse E 600 POL, at a 1000× magnification using both parallel and crossed nicols. The applied taxonomic frameworks are based upon Aubry (1984, 1988, 1989, 1990, 1999), Perch-Nielsen (1985) and Bown (1998 and references therein).

Quantitative analyses were performed for the samples collected from the Sub-Grybów Beds, Grybów Marl Formation and Krosno Beds, exposed in the second trust-sheet along the Górnikowski and Chełmski streams (Figs. 2 and 3), using counts of 300 specimens per slide. In order to analyse and calculate the percentage abundance of autochthonous and allochthonous assemblages the 5 % range error was accepted. The nominal values are presented in Tables 1 and 2.

To distinguish reworked from in-place nannofossils the full stratigraphic ranges of species, were used. Individual species older than the youngest assemblage were identified as reworked taxa. Issues do appear, especially concerning long-ranging Cenozoic taxa such *Braarudosphaera bigelowii*,

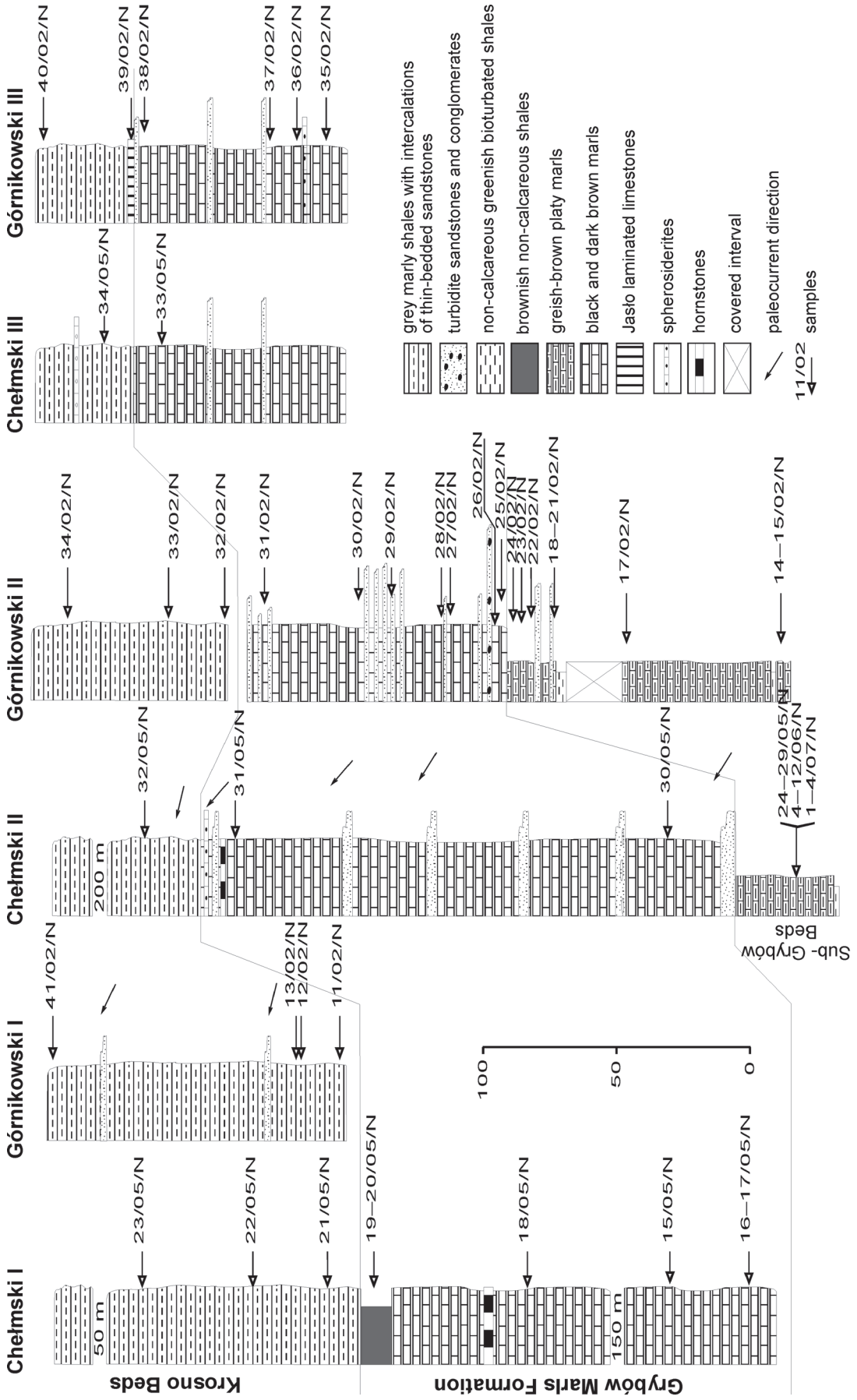

Fig. 3. Lithostratigraphic logs of the Grybów Nappe in the Ropa tectonic window (Oszczypko-Clowes 2008).

Table 1: Nominal and percentage distribution of calcareous nannoplankton in Chełmski section. × — species too rare to be included in count.

CHEŁMSKI STREAM THRUST, SHEET II																														
Lithostratigraphical units	**Sub-Grybów Beds (S-GB)**																**Grybów Marl Formation (GMF)**											**Krosno Beds**			
Sample number	**26/05/N (%)**		**27/05/N (%)**		**11/06/N (%)**		**28/05/N (%)**		**10/06/N (%)**		**9/06/N (%)**		**8/06/N (%)**		**7/06/N (%)**		**6/06/N (%)**		**5/06/N (%)**		**4/06/N (%)**		**29/05/N (%)**		**30/05/N (%)**		**31/05/N (%)**		**32/05/N (%)**	
Coronocyclus nitescens															1	0.3							1	0.32			1	0.32		
Cyclicargolithus abisectus	29	9.18	78	24.70	57	18.05	80	25.33	45	14.25	43	13.62	36	11.40	38	12.03	34	10.77	36	11.40	38	12.03	30	9.50	44	13.93	47	14.88	50	15.83
Cyclicargolithus floridanus	96	30.40	73	23.12	66	20.90	61	19.32	71	22.48	45	14.25	51	16.15	47	14.88	35	11.08	51	16.15	27	8.55	60	19.00	42	13.30	50	15.83	43	13.62
Dictyococcites bisectus	61	19.32			36	11.40	27	8.55	15	4.75	39	12.35	39	12.35	52	16.47	47	14.88	54	17.10	122	38.63	41	12.98	39	12.35	52	16.47	47	14.88
Discoaster deflandrei															2	0.63	1	0.32												
Ericsonia fenestrata			1	0.32	2	0.63									x										1	0.32				
Helicosphaera compacta		0.00	1	0.32	1	0.32	1	0.32	2	0.63		0.00	2	0.63	1	0.32	1	0.32		0.00	x		2	0.63		0.00		0.00		
Helicosphaera euphratis					3	0.95											1	0.32	1	0.32							1	0.32	1	0.32
Helicosphaera recta							1	0.32							2	0.63			x						2	0.63			x	
Pontosphaera multipora			2	0.63	1	0.32	4	1.27	1	0.32	2	0.63	1	0.32																
Reticulofenestra lockerii	5	1.58	6	1.90	4	1.27			3	0.95			x		1	0.32	7	2.22	2	0.63			3	0.95	2	0.63	2	0.63	2	0.63
Reticulofenestra minuta	22	6.97	31	9.82	29	9.18	19	6.02	14	4.43	21	6.65	24	7.60	25	7.92	25	7.92	29	9.18	40	12.67	21	6.65						
Reticulofenestra ornata			2	0.63					2	0.63	1	0.32					1	0.32	3	0.95			1	0.32			4	1.27	3	0.95
Sphenolithus dissimilis			3	0.95			5	1.58			2	0.63	1	0.32			8	2.53	5	1.58			7	2.22					5	1.58
Transversopontis obliquipons		0.00		0.00		0.00		0.00		0.00	2	0.63	1	0.32	1	0.32	1	0.32		0.00		0.00		0.00	1	0.32	x			0.00
autochthonous species	**213**	**67.45**	**197**	**62.38**	**199**	**63.02**	**198**	**62.70**	**153**	**48.45**	**155**	**49.08**	**155**	**49.08**	**170**	**53.83**	**161**	**50.98**	**181**	**57.32**	**227**	**71.88**	**166**	**52.57**	**131**	**41.48**	**157**	**49.72**	**151**	**47.82**
Zygrhablithus bijugatus	7	2.22	5	1.58	11	3.48	10	3.17	12	3.80	19	6.02	17	5.38	17	5.38	12	3.80	10	3.17	18	5.70	3	0.95	14	4.43	12	3.80	12	3.80
Braarudosphaera bigelowii			2	0.63									3	0.95	4	1.27							1	0.32						
Coccolithus pelagicus	41	12.98	59	18.68	55	17.42	63	19.95	103	32.62	90	28.50	80	25.33	75	23.75	99	31.35	82	25.97	28	8.87	83	26.28	125	39.58	103	32.62	105	33.25
Sphenolithus moriformis	7	2.22	2	0.63	5	1.58	2	0.63	3	0.95	11	3.48	16	5.07	5	1.58			1	0.32			21	6.65	3	0.95	2	0.63	3	0.95
long-ranging species	**55**	**17.42**	**68**	**21.53**	**71**	**22.48**	**75**	**23.75**	**118**	**37.37**	**120**	**38.00**	**116**	**36.73**	**101**	**31.98**	**111**	**35.15**	**93**	**29.45**	**46**	**14.57**	**108**	**34.20**	**142**	**44.97**	**117**	**37.05**	**120**	**38.00**
Chiasmolithus bidens															1	0.32														
Chiasmolithus grandis	1	0.32											1	0.32	2	0.63													4	1.27
Coccolithus eopelagicus			3	0.95	1	0.32	3	0.95	2	0.63	4	1.27	4	1.27	4	1.27	2	0.63			4	1.27					4	1.27	4	1.27
Cyclicargolithus luminis					2	0.63					1	0.32			1	0.32	1	0.32	3	0.95			2	0.63	3	0.95				
Discoaster barbadiensis											1	0.32			x								1	0.32						
Discoaster lodoensis	x		1	0.32			1	0.32	1	0.32	2	0.63																		
Discoaster tanii nodifer																									4	1.27				
Ericsonia formosa	2	0.63			1	0.32	x		2	0.63	1	0.32	1	0.32	1	0.32	4	1.27	5	1.58	2	0.63	4	1.27	2	0.63	2	0.63	2	0.63
Helicosphaera bramlettei			2	0.63											x				1	0.32					1	0.32				
Helicosphaera papillata																									x					
Helicosphaera reticulata							1	0.32																						
Isthmolithus recurvus	6	1.90			1	0.32	1	0.32											1	0.32	1	0.32			3	0.95	1	0.32	1	0.32
Lanternithus minutus	5	1.58					6	1.90	6	1.90			5	1.58	7	2.22	4	1.27	2	0.63	2	0.63			1	0.32	2	0.63	2	0.63
Neococcolithes dubius							1	0.32	1	0.32			1	0.32							1	0.32					1	0.32	1	0.32
Pontosphaera plana	x		1	0.32	2	0.63							1	0.32	x		1	0.32	1	0.32	1	0.32	1	0.32	x		1	0.32	1	0.32
Reticulofenestra dictyoda			2	0.63	4	1.27			3	0.95	2	0.63	2	0.63	2	0.63							1	0.32	2	0.63				
Reticulofenestra hillae	2	0.63	3	0.95	1	0.32					1	0.32	3	0.95	1	0.32	2	0.63			1	0.32					1	0.32	1	0.32
Reticulofenestra reticulata																					x						x		x	
Reticulofenestra umbilica	3	0.95	3	0.95													1	0.32												
Sphenolithus pseudoradians			x														2	0.63	1	0.32										
Sphenolithus radians					1	0.32	1	0.32			1	0.32							2	0.63	1	0.32					1	0.32	1	0.32
Transversopontis fibula			x																											
Transversopontis latus			x																											
Transversopontis pulcher					x																									
Cretaceous species undivided	13	4.12	20	6.33	17	5.38	13	4.12	14	4.43	12	3.80	11	3.48	10	3.17	11	3.48	10	3.17	14	4.43	17	5.38	11	3.48	13	4.12	12	3.80
reworked species	**32**	**10.13**	**35**	**11.08**	**30**	**9.50**	**27**	**8.55**	**29**	**9.18**	**25**	**7.92**	**29**	**9.18**	**29**	**9.18**	**28**	**8.87**	**26**	**8.23**	**27**	**8.55**	**26**	**8.23**	**27**	**8.55**	**26**	**8.23**	**29**	**9.18**
SUM	300	95	300	95	300	95	300	95	300	95	300	95	300	95	300	95	300	95	300	95	300	95	300	95	300	95	300	95	300	95

Table 2: Nominal and percentage distribution of calcareous nannoplankton in Górnikowski sections. × — species too rare to be included in count.

GÓRNIKOWSKI STREAM THRUST, SHEET II																														
Lithostratigraphical units	**Sub-Grybów Beds (S-GB)**																**Grybów Marl Formation (GMF)**											**Krosno Beds**			
Sample number	**14/02/N (%)**		**15/02/N (%)**		**17/02/N (%)**		**18/02/N (%)**		**19/02/N (%)**		**21/02/N (%)**		**22/02/N (%)**		**23/02/N (%)**		**26/02/N (%)**		**27/02/N (%)**		**29/02/N (%)**		**30/02/N (%)**		**31/02/N (%)**		**32/02/N (%)**		**34/02/N (%)**	
Coronocyclus nitescens	4	1.27			3	0.95	1	0.32									1	0.32												
Cyclicargolithus abisectus	15	4.75	33	10.45	19	6.02	40	12.67	142	44.97	36	11.40	23	7.28	45	14.25	38	12.03	41	12.98	51	16.15	39	12.35	50	15.83	40	12.67	44	13.93
Cyclicargolithus floridanus	27	8.55	25	7.92	38	12.03	66	20.90	7	2.22	45	14.25	39	12.35	41	12.98	44	13.93	92	29.13	88	27.87	86	27.23	39	12.35	16	5.07	57	18.05
Dictyococcites bisectus	54	17.10	89	28.18	47	14.88	25	7.92	83	26.28	44	13.93	58	18.37	60	19.00	59	18.68	54	17.10	55	17.42	63	19.95	60	19.00	88	27.87	71	22.48
Discoaster deflandrei	x		x		3	0.95	2	0.63	0		3	0.95	4	1.27	x		x		3	0.95	1	0.32	2	0.63	3	0.95				
Ericsonia fenestrata	1	0.32											x																1	0.32
Helicosphaera compacta	x						3	0.95															1	0.32					x	
Helicosphaera euphratis	1	0.32	x		1	0.32															1	0.32	2	0.63	x				x	
Helicosphaera recta	x		x		2	0.63	3	0.95																						
Pontosphaera multipora			1	0.32			2	0.63									x													
Reticulofenestra lockerii	2	0.63	3	0.95			2	0.63			3	0.95	2	0.63	4	1.27	4	1.27	x				1	0.32	5	1.58	4	1.27	2	0.63
Reticulofenestra minuta			x		5	1.58																					7	2.22		
Reticulofenestra ornata	2	0.63	6	1.90	1	0.32	4	1.27			1	0.32	3	0.95	3	0.95	3	0.95			x				4	1.27	5	1.58		
Sphenolithus dissimilis	x				1	0.32					x		x				x						x							
Transversopontis obliquipons	0		1	0.32	x		x		x		x		x		x		x		x		x		x		x		x		x	
autochthonous species	**106**	**33.57**	**158**	**50.03**	**120**	**38.00**	**148**	**46.87**	**232**	**73.47**	**132**	**41.80**	**129**	**40.85**	**153**	**48.45**	**149**	**47.18**	**190**	**60.17**	**196**	**62.07**	**194**	**61.43**	**161**	**50.98**	**160**	**50.67**	**175**	**55.42**
Braarudosphaera bigelowii																														
Coccolithus pelagicus	103	32.62	65	20.58	94	29.77	87	27.55	4	1.27	85	26.92	98	31.03	91	28.82	97	30.72	77	24.38	52	16.47	44	13.93	91	28.82	87	27.55	56	17.73
Sphenolithus moriformis	13	4.12	15	4.75	7	2.22	9	2.85	12	3.80	8	2.53	11	3.48	7	2.22		0.00	1	0.32	7	2.22	12	3.80	4	1.27	4	1.27	9	2.85
Zygrhablithus bijugatus	15	4.75	12	3.80	9	2.85	6	1.90	11	3.48	22	6.97	27	8.55	12	3.80	20	6.33	5	1.58	16	5.07	17	5.38	15	4.75	4	1.27	19	6.02
long-ranging species	**131**	**41.48**	**92**	**29.13**	**110**	**34.83**	**102**	**32.30**	**27**	**8.55**	**115**	**36.42**	**136**	**43.07**	**110**	**34.83**	**117**	**37.05**	**83**	**26.28**	**75**	**23.75**	**73**	**23.12**	**110**	**34.83**	**95**	**30.08**	**84**	**26.60**
Chiasmolithus bidens	x		x																											
Chiasmolithus grandis	1	0.32	x		1	0.32	1	0.32									4	1.27	1	0.32	1	0.32	2	0.63	2	0.63	5	1.58	2	0.63
Coccolithus eopelagicus			2	0.63	x		4	1.27			3	0.95	1	0.32	4	1.27	4	1.27	9	2.85	2	0.63	3	0.95	3	0.95	3	0.95	2	0.63
Cyclicargolithus luminis	6	1.90			1	0.32	1	0.32																						
Discoaster barbadiensis	1	0.32			1	0.32	5	1.58			1	0.32									x									
Discoaster lodoensis	x				x																									
Discoaster tanii							1	0.32																						
Discoaster tanii nodifer					2	0.63																								
Ericsonia formosa	2	0.63			2	0.63	3	0.95			1	0.32			1	0.32					3	0.95	1	0.32	3	0.95	3	0.95	1	0.32
Helicosphaera bramlettei							1	0.32																						
Helicosphaera papillata	x																													
Helicosphaera reticulata	x																													
Isthmolithus recurvus	6	1.90	11	3.48	3	0.95	5	1.58	2	0.63	2	0.63	1	0.32	1	0.32	1	0.32	1	0.32	2	0.63	2	0.63	1	0.32	3	0.95	3	0.95
Lanternithus minutus	15	4.75	22	6.97	19	6.02	13	4.12	6	1.90	22	6.97	10	3.17	17	5.38	6	1.90	2	0.63			2	0.63	2	0.63				
Neococcolithes dubius	x				3	0.95																								
Pontosphaera plana							x																							
Reticulofenestra dictyoda	7	2.22	5	1.58	4	1.27	2	0.63			3	0.95	5	1.58	1	0.32	3	0.95			1	0.32	2	0.63	2	0.63			2	0.63
Reticulofenestra hillae	1	0.32			2	0.63	5	1.58							1	0.32	2	0.63			2	0.63	1	0.32						
Reticulofenestra reticulata	7	2.22			5	1.58									1	0.32							2	0.63			2	0.63	4	1.27
Reticulofenestra umbilica	x				1	0.32					x						x				1	0.32	1	0.32						
Sphenolithus pseudoradians	1	0.32																									2	0.63	1	0.32
Sphenolithus radians	3	0.95			1	0.32			2	0.63	1	0.32	2	0.63			1	0.32	1	0.32	x		1	0.32			2	0.63		
Transversopontis fibula					x																									
Transversopontis latus			x																											
Transversopontis pulcher			x														2	0.63					2	0.63	2	0.63				
Cretaceous species undivided	13	4.12	10	3.17	25	7.92	9	2.85	31	9.82	20	6.33	16	5.07	11	3.48	11	3.48	13	4.12	17	5.38	14	4.43	14	4.43	25	7.92	26	8.23
reworked species	**63**	**19.95**	**50**	**15.83**	**70**	**22.17**	**50**	**15.83**	**41**	**12.98**	**53**	**16.78**	**35**	**11.08**	**37**	**11.72**	**34**	**10.77**	**27**	**8.55**	**29**	**9.18**	**33**	**10.45**	**29**	**9.18**	**45**	**14.25**	**41**	**12.98**
sum	**300**	**95**	**300**	**95**	**300**	**95**	**300**	**95**	**300**	**95**	**300**	**95**	**300**	**95**	**300**	**95**	**300**	**95**	**300**	**95**	**300**	**95**	**300**	**95**	**300**	**95**	**300**	**95**	**300**	**95**

Cyclicargolithus floridanus, *Coccolithus pelagicus* and *Sphenolithus moriformis*. These were counted as separate group. In such a situation the calculated percentage value of reworking should be interpreted as the minimum level of reworking.

Representative samples of marls, clay shales and turbiditic mudstones differing in colour (black, brownish, olive-green and grey) were chosen for mineralogical and petrological investigations. The mineral composition of rocks was determined using X-ray diffraction (XRD). Fourteen samples of rock were ground before testing in a ceramic mortar. The analyses were performed using a Philips X'Pert diffractometer with the generator PW1870 and the vertical goniometer PW3020, equipped with a graphite diffracted-beam monochromator. CuKα radiation was used with the applied voltage of 40 kV and 30 mA current. The random mounts were scanned from 2–64° 2Θ at a counting time of 1 second per 0.02° step.

Petrological features were studied in thin-sections of 13 samples by using optical microscopy Nikon-Eclipse E 600 POL, under transmitted light. The XRD and optical analyses were performed at the Institute of Geological Sciences, Jagiellonian University, Kraków, Poland. The abbreviations for names of rock-forming minerals follow Whitney & Evans (2010). Thirty samples of pelite rocks from the Ropa tectonic window were selected for geochemical studies. Samples were collected from each of the three thrust-sheets. They represent a complete sequence from the S-GB through the GMF to the Krosno Beds. Similar lithotypes were used for comparison. Many data reflect chemical variations in each lithology. The rock samples were crushed and hand-pulverized in agate mortar and pestle to the fraction passing 200 mesh. Sample amounts of typically 0.2 g dry weight pulp were decomposed by lithium borate fusion and dilute acid digestion before a classical whole-rock analysis by ICP emission spectrometry. ICP-OES analyses of major oxides package includes SiO_2, Al_2O_3, Fe_2O_3, MgO, CaO, Na_2O, K_2O, TiO_2, P_2O_5, MnO, Cr_2O_3 and loss on ignition (LOI), which is measured by weight difference after ignition at 1000 °C. Trace element contents were determined through the ICP-MS technique (ACME Analytical Laboratories, Ltd., 2013). Geochemical analyses were conducted at the ACME Laboratory in Vancouver, Canada.

Contents of major, minor and trace elements in the studied material were compared to those in the standard sediments: Post-Archean Australian Shale (PAAS after Taylor & McLennan 1985), average shales (Wedepohl 1991) and upper continental crust (UCC — after Rudnick & Gao 2003; Hu & Gao 2008). The Eu anomaly expressed by Eu/Eu* ratio was calculated using $Eu/Eu^* = Eu_N/(Sm_N \times Gd_N)^{0.5}$ ratio, where $_N$ means element content normalized to UCC. The Ce anomaly was calculated analogous, using the ratio $Ce/Ce^* = Ce_N/(La_N \times Pr_N)^{0.5}$.

The A–CN–K triangular plot is based on the ratio between Al_2O_3, $CaO^* + Na_2O$ and K_2O (Nesbitt & Young 1984). CaO* is the amount of CaO in the silicate fraction. If CaO has affinity to carbonates, CaO* is equivalent to Na_2O (McLennan 1993; cf. Hofer et al. 2013). The chemical index of alteration (CIA — Nesbitt & Young 1982) is used to determine the degree of source area weathering. The formula for calculating the CIA is as follows:

$CIA = (Al_2O_3/Al_2O_3 + Na_2O + K_2O + CaO)*100$.

The chemical proxy of alteration (CPA; Cullers 2000) was used as a complement to the CIA when it is affected by CaO from minerals other than silicates. The CPA is calculated as follows:

$CPA = (Al_2O_3/(Al_2O_3 + Na_2O))*100$.

Results

Calcareous nannofossils

Preservation and abundance

State of preservation is one of the methods used in identifying reworked fossils via the presence of very intensive mechanical damage as well as signs of etching, severe dissolution and overgrowth. When considering all the investigated assemblages the preservation of calcareous nannofossils is moderate (m) or predominantly moderate-to-good (m-g) in all investigated samples (Tables 1 and 2). Nannofossils show minor etching and minor-to-moderate over growth. A good to moderate preservation of nannofossils indicates that little carbonate dissolution has occurred in these sediments.

Biostratigraphy

Analyses, using the standard Martini zonation (1971), confirmed results obtained through earlier research (Oszczypko-Clowes 2008). The obtained results for all the samples from Ropa tectonic windows, are summarized in Table 3.

The FO of *Cyclicargolithus abisectus* is usually found close to the FO of *Sphenolithus ciperoensis* (zonal marker for the lower boundary of NP24 Zone) and thus can be used to approximate the boundary of NP23 and NP24 (Martini & Műller 1986). However, many authors believed that this species is already present in the lower part of the NP23 (e.g. Bukry 1973; de Kaenel & Villa 1996; Melinte 2005; Maiorano & Monechi 2006; Melinte-Dobrinescu & Brustur 2008). The size of coccolith is important, smaller sizes are characteristic of the upper part of NP23 and NP24, greater (greater than 10 or 11 microns, see e.g. De Kaenel & Villa 1996; Maiorano & Monechi 2006; Śliwińska et al. 2012) for the upper part of NP24.

Taking into account the absence of *Transversopontis fibula*, *Orthozygus aureus*, *Lanternitus minutus* and *Chiasmolithus oamaruensis*, which has the LO in the upper part of NP23 (see Melinte 2005) it is possible to include the given samples into NP24 Zone. In addition, *Sphenolithus dissimilis* Bukry & Percival was also observed. The FO of these species is characteristic for zone NP24 (see Perch-Nielsen 1985). However the size of *Cyclicargolithus abisectus* varies. *C. abisectus* found in assemblages belonging to the Sub-Grybów Beds were smaller than 10 microns, which can indicate the lower part of NP24, whereas assemblages from the Grybów Marl Formation and Krosno Beds contained specimens bigger than 10 microns. This indicates the upper part of NP24.

Table 3: Biostratigraphy based on calcareous nannofossils (based on Oszczypko-Clowes 2008).

ROPA — CHEŁMSKI STREAM					
THRUST SHEET I		**THRUST SHEET II**			**THRUST SHEET III**
Grybów Marl Formation (GMF)	Krosno Beds	Sub-Grybów Beds (S-GB)	Grybów Marl Fm (GMF)	Krosno Beds	GMF
NP24	NP24 and NP25	NP24	NP24	NP24	NP24

ROPA — GÓRNIKOWSKI STREAM					
THRUST SHEET I	**THRUST SHEET II**			**THRUST SHEET III**	
Krosno Beds	Sub-Grybów Beds (S-GB)	Grybów Marl Fm (GMF)	Krosno Beds	GMF	Krosno Beds
NP25	NP24	NP24	NP24	NP24	NP24

The zone assignment of NP25 is based on the first occurrence (FO) of *Sphenolithus capricornutus* and *S. conicus*. Slightly less abundant are *Cyclicargolithus abisectus*, *Reticulofenestra lockeri*, *S. dissimilis* and *R. dictyoda*. *Dictyococcites bisectus* is present, though rare. The FO of *Sphenolithus conicus* has been frequently used as the base of the NN1 zone, however, Bizon & Műller (1979), Biolzi et al. (1981) and Melinte (1995) observe the FO of this species as low as the upper part of the NP25 zone. This zone was determined in thrust-sheet I of both sections, within the Krosno beds.

Species diversity and age determination of reworked assemblages

Forty four species were identified during quantitative analyses of calcareous nannoplankton. The difference between the reworked assemblages of the two sections has only a quantitative character. Qualitatively these assemblages are the same. The level of reworking is generally not too high. It varies from 8 % to 11 % for the samples collected from the Chełmski section and from 9 % up to 17 % in the case of the Górnikowski section (Fig. 4, Tables 1 and 2). The exceptions are samples 14/02/N and 17/02/N where the level of reworking reaches the value of 20 % and 22 % respectively. The greatest number of reworked specimens was observed in samples 27/05/N and 26/05/N (11 % and 10 %, respectively) taken from the Sub-Grybów Beds.

The reworked assemblage consists of Paleogene and Cretaceous taxa. In the Chełmski section the Cretaceous species form between 3 % and 6 % of the reworked association whereas in the case of the Górnikowski section it is between 3 % and 8 %, except for the sample 19/02/N with the value of 10 % (Tables 1 and 2, Fig. 4). The percentage abundance of Paleogene species varies from 3 % up to 6 % (Chełmski section) and from 3 % up to 16 % (Górnikowski section). The main components of the Paleogene assemblage (Tables 1 and 2) are *Reticulofenestra* spp., *Isthmolithus recurvus*, and *Lanternithus minutus*. *Reticulofenestra* spp. ranges from 0 (samples 28/05/N and 5/06/N — Chełmski section; 19/02/N and 27/02/N — Górnikowski section) up to 3 % (sample 27/05/N — Chełmski section) and 5 % (14/02/N — Górnikowski section). The abundance of *Isthmolithus recurvus* does not exceed 2 % in the case of the Chełmski section, whereas in the case of Górnikowski section it is higher, approaching the value of 5 % (sample 15/02/N). The most abundant element of the assemblage is *Lanternithus minutus.* The average content of this species for the Górnikowski section is 3 %. In the Chełmski section it is much lower with the result that 4 samples out of 15 did not contain *Lanternithus minutus* (Tables 1 and 2).

The precise age determination of Paleogene assemblages is not easy, especially as an overlap pattern of several index species is visible. The only typical Lower Eocene taxon is *Discoaster lodoensis* (NP12–14). The most abundant are long-ranging species including *Discoaster barbadiensis* (NP10–20), *Ericsonia formosa* (NP21), *Helicosphaera bramlettei* (NP14–23) *Lanternithus minutus* (NP16–22), *Reticulofenestra hillae* (NP16–22) and *R. umbilica* (NP16–22).

Their stratigraphic ranges span from the Middle Eocene to Early Oligocene. These taxa may constitute Middle Eocene, Late Eocene or even Early Oligoceene assemblages. The presence of Middle Eocene could be dated by the *Chiasmolithus grandis* (NP11–17).

The presence of *Isthmolithus recurvus* suggests that part of the assemblage may be not older than Zone NP19–20 (Late Eocene) and not younger than NP22 (Early Oligocene), as *R. umbilica* is the index species for the upper limit of Zone NP22).

Mineralogy and geochemistry

Mineral composition and petrographic features

The mineral composition of the material studied was carried out using X-ray diffraction. All of the samples studied consist of quartz, feldspar, 10 Å-phyllosilicates (mica) and clay minerals (mixed-layer I/S, kaolinite and chlorite). Quartz peaks are the most intensive in the mudstone samples. Taking into account the calcite content, the Grybów Marl Formation is the most enriched, whereas the Krosno Beds are destitute of calcite. The XRD pattern of the marl samples of the GMF (e.g. 17/05/N, 30/05/N, 33/05/N) weakly register the peaks of clay minerals. However, the kaolinite peak is always evident. Some mudstones and marly shales of the S-GB and GMF (e.g. samples 18/02/N, 19/02/N, 35/02/N, 24/02/N and 33/05/N) display intensive peaks of Mg-Fe carbonates on the XRD pattern (Fig. 5).

Rhombohedra of carbonate minerals were microscopically noted in many samples (e.g. 1/07/N, 26/05/N, 33/05/N). The thin-section examinations reveal discrete lamination emphasized by parallel lying mica flakes and strips of organic matter. The S-GB and GMF contain abundant glauconite, whose contents decrease in the Krosno Beds. Heavy minerals represented by abraded grains of zircon, rutile and tourmaline were recognized in the silt and mudstone samples (1/07/N, 19/05/N, 20/02/N, 33/05/N; Fig. 6) and also in the clayey

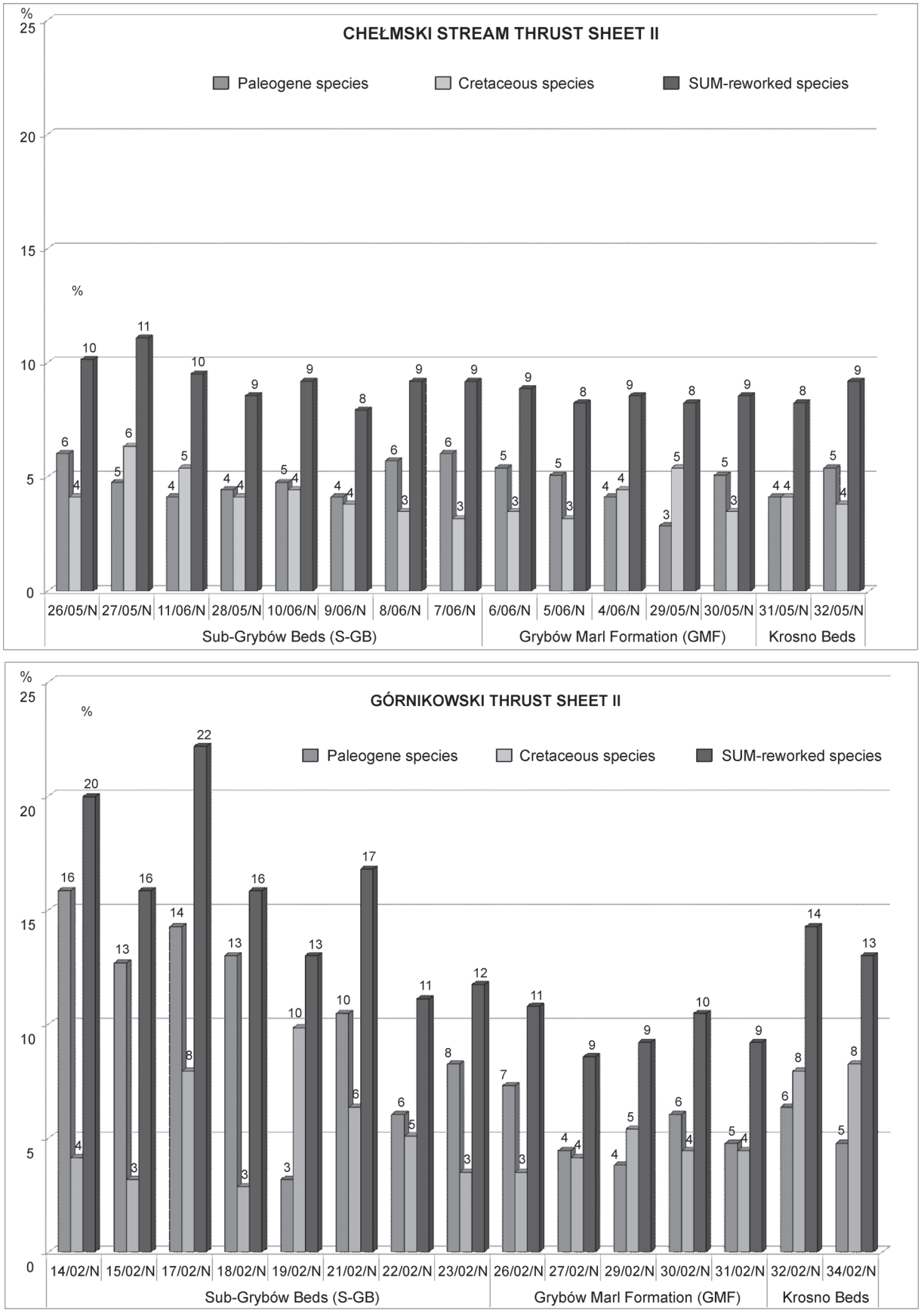

Fig. 4. Percentage abundance of allochthonous species in samples.

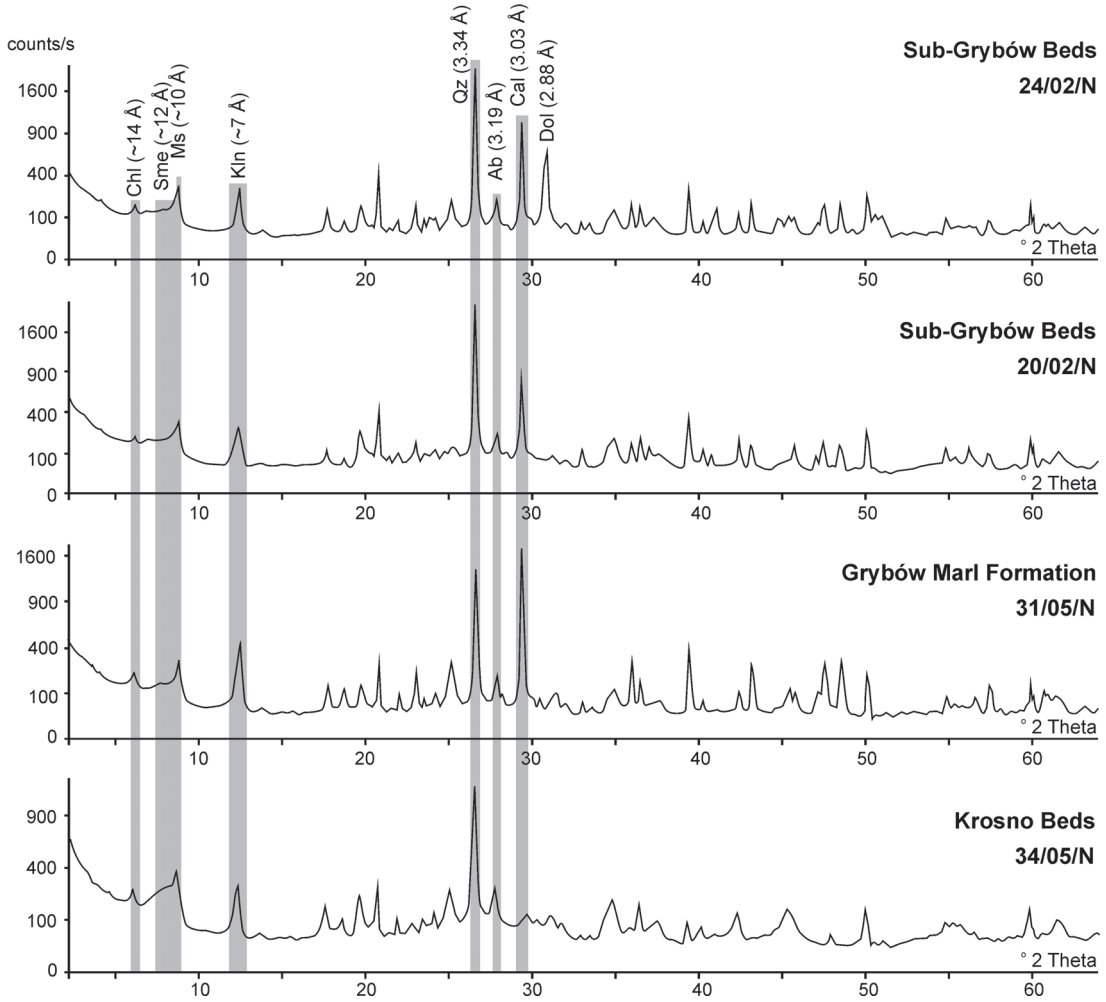

Fig. 5. The powder XRD patterns of samples representing the Sub-Grybów Beds, Grybów Marl Formation and Krosno Beds of the Grybów Nappe from the Ropa tectonic windows. **Ab** — albite, **Cal** — calcite, **Chl** — chlorite, **Dol** — dolomite, **Kln** — kaolinite, **Ms** — muscovite, **Qz** — quartz, **Sme** — smectite.

shales (24/05/N). Organic matter, an important component of the black and brownish samples, is comprised mainly of the remains of plants. The black detritus occurs abundantly in the dark samples (e.g. 1/07/N, 16/05/N, 19/05/N; Fig. 6) and, with a lesser frequency, in the light-coloured samples (26/05/N, 28/05/N, 20/02/N). Organic matter is associated with pyrite which is often transformed into amorphous Fe oxyhydroxides (Fig. 6).

Chemical composition

Major elements

Major element compositions of the Grybów Unit samples are shown in Table 4. The average compositions of Upper Continental Crust (UCC — Rudnick & Gao 2003; Hu & Gao 2008), Post-Archean Australian Shale (PAAS — Taylor & McLennan 1985) and average shales are also listed for comparison. Major element abundances in formations studied are usually lower than that in standards, except for CaO, contents of which are significantly higher in the samples. Owing to the strongly calcareous character of the sediments, CaO dilutes other chemical components. Samples 18/02/N and 24/05/N from the Sub-Grybów Beds contain SiO_2, Al_2O_3 and CaO in amounts comparable to these of the average shales. Few samples of moderately calcareous shales and mudstones of the S-GB (18/02/N, 20/02/N, 1/07/N, 24/05/N) and the Krosno Beds (34/05/N) resemble the average shales in respect of contents of Al_2O_3 or SiO_2. Certain samples of the S-GB (19/02/N, 24/02/N, 24/05/N) and the GMF (16/05/N) from the second thrust-sheet are enriched in Fe_2O_3 relative to the standards. The samples 1/07/N, 18/02/N and 24/02/N are also rich in MgO. The highest amounts of MgO were recognized in two samples 35/02/N and 32/02/N of the GMF and Krosno Beds, respectively.

High field strength trace elements (Zr, Hf, Nb) and Th, U, REE

The concentrations of trace elements (TE) in the samples of the Grybów Nappe from the Ropa tectonic window are shown in Table 4. The material studied is generally depleted of TE relative to the upper continental crust (UCC) and Post-

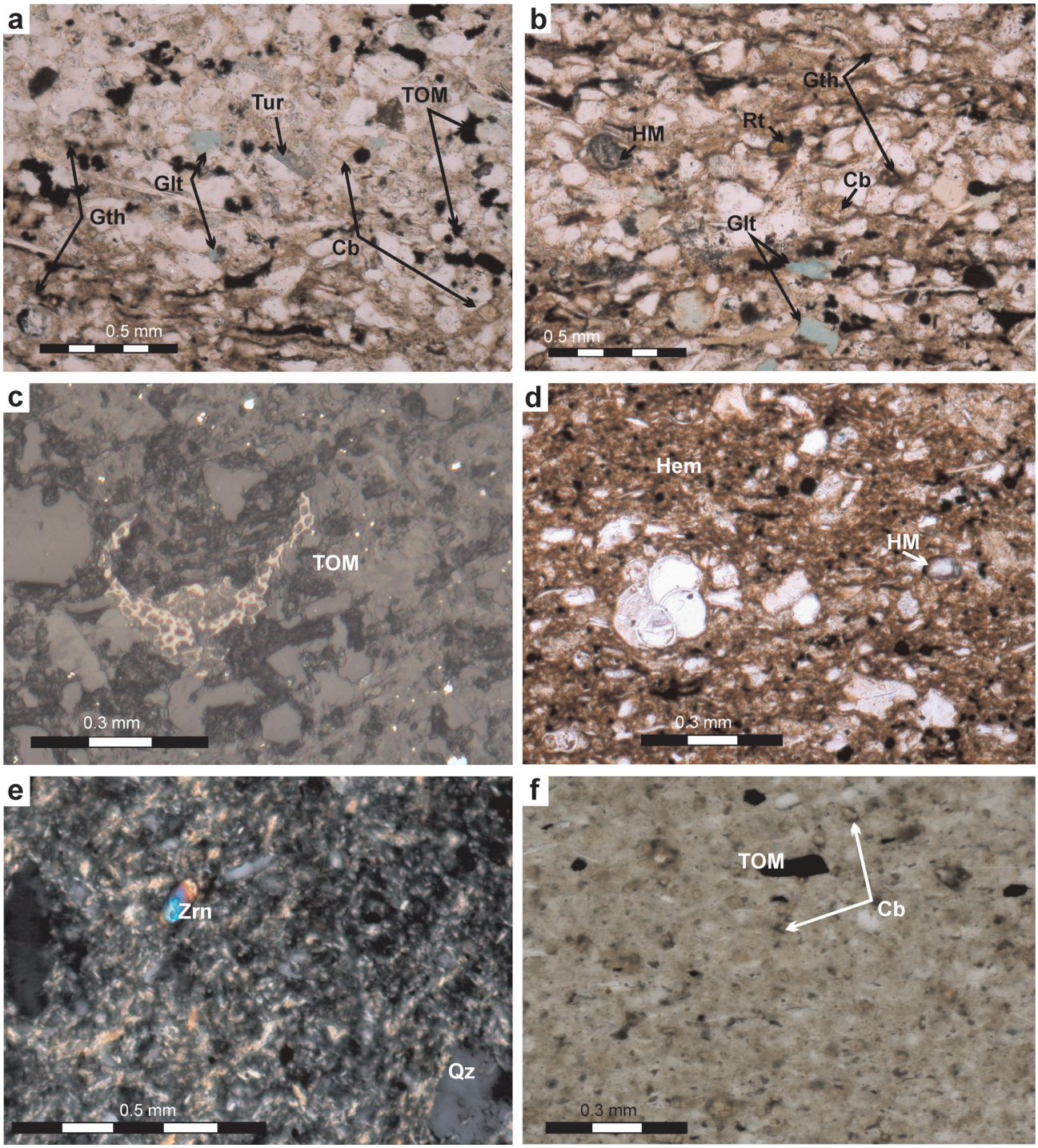

Fig. 6. Thin-section microphotographs showing recycled specimens. **a, b** — silt-grained sample of the Sub-Grybów Beds 1/07/N, transmitted light (TL), parallel polars; **c** — black mudstones of the GMF, sample 19/05/N, reflected light; **d** — black mudstones of the GMF, sample 19/05/N, TL, parallel polars; **e** — bluish-grey clayey shale of the S-GB, sample 24/05/N, TL, crossed polars; **f** — green marly shale of the S-GB, sample 26/05/N, TL, parallel polars. **Cb** — carbonate minerals, **Glt** — glauconite, **Ght** — goethite, **Hem** — hematite, **HM** — heavy minerals (undefined), **Qz** — quartz, **Rt** — rutile, **TOM** — terrestrial organic matter, **Zrn** — zircon.

Archean Australian shales (PAAS). Th and Nb mostly correlate with TiO_2 and Al_2O_3 (Fig. 7). The higher concentrations of TiO_2, Th and Nb are found in the samples from the S-GB (24/05/N and 18/02/N) and Krosno Beds (34/05/N) that contain the highest amounts of Al_2O_3. TiO_2 co-occurring with Zr and Y correlate positively also with SiO_2 (Fig. 7, Table 4). It is particularly visible in the silt samples of the S-GB (20/02/N and 1/07/N). Accumulation of TE and SiO_2 also occurs in the samples of the S-GB and Krosno Beds (24/05/N and 34/05/N) that are concomitantly enriched in Al_2O_3 (Table 4).

Table 4: Whole-rock major, minor, and rare-earth element abundances for the Sub-Grybów Beds, Grybów Marl Formation and Krosno Beds of the Grybów Nappe from the Ropa Grybów tectonic window. UCC data from Rudnick & Gao (2003) and Hu & Gao (2008); Post-Archean Australian Shale (PAAS) — Taylor & McLennan 1985).

			Chełmski I						Chełmski II						Górnikowski II						
Lithostratigraphical units			Grybów Marl Formation					Kr. B.	Sub-Grybów Beds				Grybów Marl Fm		Sub-Grybów Beds						
Nannoplankton zones			24	24	24	24	24	24		24	24	24	24	24	24	24	24	24	24	24	
Sample number			16/05/N	15/05/N	18/05/N	19/05/N	20/05/N	21/05/N	1/07	24/05/N	26/05/N	28/05/N	30/05/N	31/05/N	18/02/N	19/02/N	20/02/N	21/02/N	22/02/N	23/02/N	24/02/N
SiO_2	%	0.01	35.76	28.18	39.44	37.33	50.51	45.91	62.87	58.21	39.28	40.18	41.60	38.90	52.36	38.37	57.43	43.85	41.62	36.96	46.92
Al_2O_3	%	0.01	11.92	9.24	13.16	12.26	12.33	13.06	8.10	18.68	13.62	13.45	13.19	13.76	15.83	10.54	13.18	13.66	13.51	12.83	13.17
Fe_2O_3	%	0.04	7.44	3.67	6.40	4.88	5.60	4.14	7.88	6.78	4.49	5.17	5.66	5.96	6.93	7.61	6.43	6.12	5.81	5.83	6.70
MgO	%	0.01	1.45	1.51	2.73	1.55	1.23	2.28	1.60	2.82	1.87	2.01	1.89	2.35	3.27	2.43	2.12	2.94	2.90	2.32	3.03
CaO	%	0.01	16.50	27.81	15.51	17.44	8.99	13.58	7.67	0.60	18.15	17.33	15.09	17.02	5.73	19.30	6.46	13.46	15.53	19.62	11.48
Na_2O	%	0.01	0.43	0.44	0.84	0.46	0.53	0.79	0.68	0.89	0.73	0.75	0.54	0.74	0.99	0.45	1.25	0.80	0.80	0.68	1.38
K_2O	%	0.01	2.12	1.75	2.52	2.17	2.40	2.67	1.26	3.76	2.87	2.76	2.70	2.71	2.92	1.63	2.32	2.80	2.82	2.40	2.25
TiO_2	%	0.01	0.55	0.38	0.63	0.61	0.57	0.67	0.66	0.83	0.58	0.59	0.58	0.60	0.78	0.39	0.73	0.67	0.66	0.58	0.76
P_2O_5	%	0.01	0.15	0.13	0.12	0.13	0.19	0.13	0.06	0.09	0.06	0.08	0.11	0.13	0.12	0.08	0.08	0.12	0.11	0.12	0.14
MnO	%	0.01	0.30	0.12	0.15	0.34	0.03	0.08	0.18	0.03	0.18	0.08	0.07	0.15	0.25	0.26	0.18	0.17	0.14	0.18	0.11
Cr_2O_3	%	0.002	0.023	0.015	0.025	0.017	0.020	0.023	0.013	0.022	0.013	0.014	0.017	0.021	0.019	0.011	0. 027	0.017	0.017	0.018	0.025
LOI	%	–5.1	23.1	26.5	18.2	22.6	17.4	16.5	8.9	7.1	17.9	17.4	18.3	17.4	10.6	18.7	9.6	15.2	15.9	18.2	13.8
CIA			80.0	77.8	75.8	79.9	78.1	75.4	75.6	77.1	75.9	75.9	77.7	76.7	76.4	80.6	73.2	75.6	75.3	77.3	72.4
CPA			96.5	95.5	94.0	96.4	95.9	94.3	92.3	95.5	94.9	94.7	96.1	94.9	94.1	95.9	91.3	94.5	94.4	95.0	90.5
Sc	ppm	1	13	10	15	12	14	12	9	19	12	13	14	15	17	10	12	15	15	14	14
Hf	ppm	0.1	3.2	2.0	3.0	3.5	3.5	4.4	9.2	4.2	2.7	3.0	3.4	2.5	4.3	1.9	5.3	3.4	3.1	3.0	3.8
Nb	ppm	0.1	10.7	7.0	10.3	11.8	11.0	13.2	13.1	15.6	10.6	11.2	11.1	10.5	14.4	7.2	13.7	13.4	12.8	9.8	13.3
Ta	ppm	0.1	0.7	0.5	0.9	0.9	0.8	1.1	0.9	1.2	0.9	1.0	0.9	0.7	1.2	0.5	1.0	1.0	1.1	0.8	1.1
Th	ppm	0.2	9.8	7.6	11.3	10.8	9.7	12.0	8.1	14.7	12.2	11.9	11.0	12.1	13.4	7.4	11.0	11.4	12.3	10.2	10.8
U	ppm	0.1	15.5	7.4	7.2	9.9	8.2	4.0	4.3	2.8	2.1	2.2	5.3	2.4	2.9	2.8	3.3	3.1	3.1	3.4	2.8
Zr	ppm	0.1	108.7	69.7	106.2	127.5	115.5	152.6	330.9	153.3	93.1	92.9	108.0	91.2	139.1	64.0	189.5	113.5	110.5	96.8	137.3
Y	ppm	0.1	23.8	17.5	22.5	25.3	24.0	22.9	32.1	24.3	18.6	16.9	24.3	20.5	24.9	26.6	22.9	23.6	22.1	21.1	20.8
La	ppm	0.1	26.8	20.7	28.1	29.2	28.4	32.2	20.9	35.8	26.1	26.0	32.0	28.4	30.2	23.8	28.2	29.9	29.3	26.5	21.7
Ce	ppm	0.1	57.9	43.6	60.5	61.8	63.1	69.7	51.6	92.5	60.3	61.2	74.0	63.0	74.0	57.9	67.7	68.9	65.2	59.1	50.4
Pr	ppm	0.02	6.35	4.81	6.54	6.74	6.74	7.56	5.18	8.65	5.93	6.02	7.63	6.69	7.36	5.62	6.82	7.19	6.94	6.28	5.46
Nd	ppm	0.3	24.3	19.0	25.8	25.2	26.0	27.5	20.0	32.5	22.3	22.5	28.0	24.8	28.1	22.1	25.6	28.2	26.1	23.3	20.6
Sm	ppm	0.05	4.86	3.61	4.75	4.95	4.79	5.02	4.57	6.11	4.10	4.22	5.41	4.53	5.54	5.05	4.52	5.34	4.83	4.53	4.18
Eu	ppm	0.02	0.99	0.77	0.99	1.03	1.05	1.00	1.18	1.21	0.88	0.88	1.13	1.02	1.14	1.29	0.95	1.12	1.00	0.99	0.89
Gd	ppm	0.05	4.17	3.06	4.28	4.51	4.29	4.19	5.12	4.76	3.32	3.41	4.77	4.12	4.85	5.32	3.87	4.72	4.11	4.09	3.79
Tb	ppm	0.01	0.68	0.52	0.70	0.75	0.69	0.70	0.94	0.78	0.57	0.55	0.75	0.67	0.80	0.87	0.67	0.78	0.70	0.65	0.64
Dy	ppm	0.05	3.89	2.67	3.85	3.89	3.71	3.78	5.20	4.35	2.96	2.84	4.16	3.55	4.45	4.63	3.79	4.26	3.85	3.53	3.52
Ho	ppm	0.02	0.76	0.57	0.73	0.80	0.75	0.76	1.04	0.86	0.62	0.60	0.82	0.70	0.86	0.85	0.74	0.82	0.77	0.70	0.72
Er	ppm	0.03	2.24	1.65	2.27	2.29	2.19	2.26	3.06	2.58	1.77	1.68	2.40	2.03	2.56	2.12	2.29	2.40	2.32	1.97	2.18
Tm	ppm	0.01	0.34	0.25	0.35	0.36	0.35	0.35	0.48	0.40	0.29	0.28	0.37	0.32	0.39	0.32	0.38	0.37	0.37	0.31	0.33
Yb	ppm	0.05	2.16	1.55	2.17	2.27	2.06	2.16	2.88	2.52	1.72	1.70	2.36	1.98	2.54	1.95	2.36	2.30	2.16	1.96	2.10
Lu	ppm	0.01	0.33	0.24	0.33	0.35	0.31	0.34	0.45	0.39	0.27	0.27	0.34	0.29	0.37	0.28	0.34	0.33	0.34	0.30	0.32
Eu/Eu*			0.92	1.31	0.92	0.87	0.96	0.89	0.95	0.78	1.22	1.15	0.82	1.03	0.80	0.90	1.02	0.84	0.95	1.00	1.06
Ce/Ce*			1.05	1.03	1.05	1.04	1.07	1.05	1.24	1.17	1.14	1.15	1.12	1.08	1.17	1.18	1.15	1.11	1.08	1.08	1.09

Table 4: *Continued.*

			Górnikowski II						Chełmski III		Górnikowski III				
Lithostratigraphical units			Grybów Marl Formation					Kr. B.	GMF	Kr. B.	GMF				
Nannoplankton zones				24	24	24	24	24	24		24	24	24		
Sample number			25/02/N	26/02/N	27/02/N	28/02/N	31/02/N	32/02/N	33/05/N	34/05/N	35/02/N	36/02/N	37/02/N	PAAS	UCC
SiO_2	%	0.01	38.71	41.75	39.29	43.65	36.06	42.13	46.19	54.89	44.54	36.92	42.77	62.8	63.5
Al_2O_3	%	0.01	12.86	13.76	12.07	15.42	13.07	12.15	13.57	21.91	14.07	13.12	12.54	18.9	15
Fe_2O_3	%	0.04	5.71	6.08	5.79	5.42	4.68	4.57	5.61	5.47	5.94	5.46	5.49	6.5	6.02
MgO	%	0.01	2.36	2.80	2.93	2.12	1.65	3.94	2.97	2.67	3.48	2.16	2.21	2.2	3.59
CaO	%	0.01	18.76	14.75	18.14	12.92	20.32	15.24	10.75	0.70	11.92	19.45	16.54	1.3	5.25
Na_2O	%	0.01	0.76	0.79	0.90	0.83	0.53	0.66	0.70	0.97	0.90	0.63	0.98	1.2	3.39
K_2O	%	0.01	2.58	2.83	2.22	3.01	2.70	2.49	2.79	5.03	2.62	2.48	2.46	3.7	2.3
TiO_2	%	0.01	0.61	0.69	0.60	0.64	0.58	0.56	0.64	0.94	0.71	0.57	0.62	1	0.69
P_2O_5	%	0.01	0.10	0.14	0.17	0.10	0.06	0.11	0.12	0.09	0.15	0.12	0.13	0.16	0.15
MnO	%	0.01	0.10	0.13	0.23	0.09	0.08	0.08	0.20	0.04	0.18	0.13	0.09	0.11	0.1
Cr_2O_3	%	0.002	0.020	0.018	0.018	0.017	0.014	0.020	0.019	0.021	0.017	0.021	0.025		
LOI	%	–5.1	17.2	16.1	17.4	15.6	20.0	17.9	16.3	7.1	15.3	18.7	15.9		
CIA			75.8	75.7	75.0	76.8	77.7	76.1	76.4	75.9	76.1	77.8	73.9		
CPA			94.4	94.6	93.1	94.9	96.1	94.8	95.1	95.8	94.0	95.4	92.8		
Sc	ppm	1	15	15	13	15	13	12	14	21	15	15	14	16	14
Hf	ppm	0.1	2.8	3.1	3.1	2.7	2.8	3.2	3.4	5.0	3.6	2.7	3.6	20	5.3
Nb	ppm	0.1	9.8	13.0	11.0	11.8	10.7	10.4	12.9	17.2	13.6	10.1	10.8	19	12
Ta	ppm	0.1	0.7	1.0	0.8	0.9	0.8	0.7	1.0	1.4	1.0	0.7	0.8		0.9
Th	ppm	0.2	11.9	11.5	9.6	12.9	11.7	9.8	11.5	17.9	11.8	11.1	10.9	14.6	10.5
U	ppm	0.1	2.9	2.7	2.7	3.1	2.3	3.5	6.1	3.4	4.3	7.2	5.8	3.1	2.7
Zr	ppm	0.1	100.2	105.9	105.8	92.6	88.1	104.8	114.8	148.2	112.9	94.2	127.0	210	193
Y	ppm	0.1	21.2	23.4	24.2	22.2	17.7	20.2	22.7	27.5	26.0	22.6	24.6	27	21.0
La	ppm	0.1	26.7	27.8	26.3	29.6	25.1	26.2	30.1	47.5	30.3	27.8	28.1	38	31
Ce	ppm	0.1	59.8	64.1	56.9	68.0	58.3	54.7	63.4	110.1	68.9	62.8	62.5	80	63
Pr	ppm	0.02	6.38	6.88	6.35	7.03	6.03	6.10	7.07	11.21	7.51	6.79	6.80	8.8	7.1
Nd	ppm	0.3	24.2	27.4	25.6	25.3	22.5	22.5	26.0	42.8	29.5	26.1	26.1	33.9	27
Sm	ppm	0.05	4.71	5.51	5.11	5.06	4.43	4.21	4.86	7.32	5.77	5.03	5.05	5.6	4.7
Eu	ppm	0.02	1.01	1.24	1.18	1.08	0.93	0.87	1.03	1.35	1.27	1.01	1.04	1.1	1
Gd	ppm	0.05	4.20	5.02	4.81	4.36	3.71	3.75	4.22	5.33	5.43	4.37	4.65	4.66	4
Tb	ppm	0.01	0.69	0.79	0.79	0.70	0.60	0.60	0.68	0.87	0.86	0.71	0.74	0.77	0.7
Dy	ppm	0.05	3.74	4.34	4.21	3.83	3.20	3.33	3.78	4.67	4.74	3.78	4.04	4.4	3.9
Ho	ppm	0.02	0.72	0.80	0.83	0.74	0.58	0.66	0.78	0.96	0.90	0.77	0.82	1	0.83
Er	ppm	0.03	2.16	2.30	2.31	2.23	1.82	1.91	2.27	2.98	2.50	2.15	2.39	2.85	2.3
Tm	ppm	0.01	0.33	0.35	0.35	0.34	0.28	0.31	0.34	0.48	0.38	0.34	0.38	0.41	0.37
Yb	ppm	0.05	2.05	2.11	2.05	2.03	1.75	1.94	2.11	3.07	2.30	2.09	2.26	2.8	2.34
Lu	ppm	0.01	0.30	0.32	0.31	0.32	0.26	0.28	0.33	0.45	0.35	0.33	0.36	0.43	0.36
Eu/Eu*			0.96	0.84	0.90	0.92	1.06	1.04	0.94	0.65	0.76	0.86	0.83		
Ce/Ce*			1.08	1.09	1.04	1.11	1.12	1.02	1.02	1.12	1.08	1.08	1.06		

An enhanced concentration of uranium, predominantly occurs in the black and brownish, marly shales of the GMF (maximal amounts of U are recognized in 15/05/N, 19/05/N, 20/05/N). Contents of U reveal no correlation with Al_2O_3 (Fig. 7).

Generally, the REE distribution in the material studied differs from that in UCC. Only two samples 22/02/N and 21/05/N from the S-GB and Krosno Beds respectively are concurrent to UCC. The distribution of REE normalized to UCC in the samples 15/05/N and 32/05/N, from the GMF and Krosno Beds respectively is parallel to that of PAAS, however the contents measured of REE are lower than that of PAAS (Fig. 8, Table 4). Most of the samples show a tendency towards decreasing heavy-REE (HREE) (Fig. 8). Two samples from the S-GB (24/02/N and 1/07/N) portray the climbing trend. The UCC normalized REE patterns of many samples (e.g. 19/02/N, 19/05/N, 27/02/N, 35/02/N, 37/02/N) show clearly convex curvatures in middle-REE (MREE) with respect to light- and heavy-REE (Fig. 8). MREE enrichment co-varying with P_2O_5 was described in the samples 27/02/N, 35/02/N, 16/05/N, 20/05/N, of which 16/05/N, 20/05/N are brown marly shales (Table 4). All these samples are concomitantly rich in MnO and Fe_2O_3 (all Fe was measured as Fe_2O_3). Some samples show MREE convex curvatures and enrichment in MnO, Fe_2O_3 and/or MgO in spite of low phosphorous content (19/05/N 18/02/N, 19/02/N, 33/05/N).

Some samples enriched in HREE also contain higher amounts of Y (19/05/N), Zr (20/02/N, 24/02/N), or both, Zr and Y (1/07/N, 18/02/N) (Table 4). Eu anomaly is slightly negative, but several samples of the S-GB (26/05/N, 28/05/N, 20/02/N, 23/02/N, 24/02/N), GMF (15/05/N, 31/05/N, 31/02/N) and Krosno Beds (32/02/N) show Eu/Eu*≥1. Correlation between Eu/Eu* and Al_2O_3 is clearly negative for the S-GB and Krosno Beds. In the GMF, Eu/Eu* changes independently from Al_2O_3. Ce anomaly is positive (Ce/Ce*>1) in all samples (Table 4). Higher values of the Ce/Ce* ratio (1.08–1.24) characterize the S-GB, whereas lower Ce/Ce*, ranging from 1.02 to 1.12 were measured in the GMF and Krosno Beds. Correlation of Ce/Ce* to Al_2O_3 is flat in the GMF. In the S-GB and Krosno Beds, Ce anomaly correlates positively with Al_2O_3 (Fig. 7).

Interpretation

Source rocks and sedimentary processes

Major element chemistry employed to determine the weathering of the source rocks can also deliver evidence of recycled material presence. In the A–CN–K diagram (Fig. 9), the samples of the Grybów Unit cluster in the upper part of the triangle, along the A–K axis, pointing to the source in

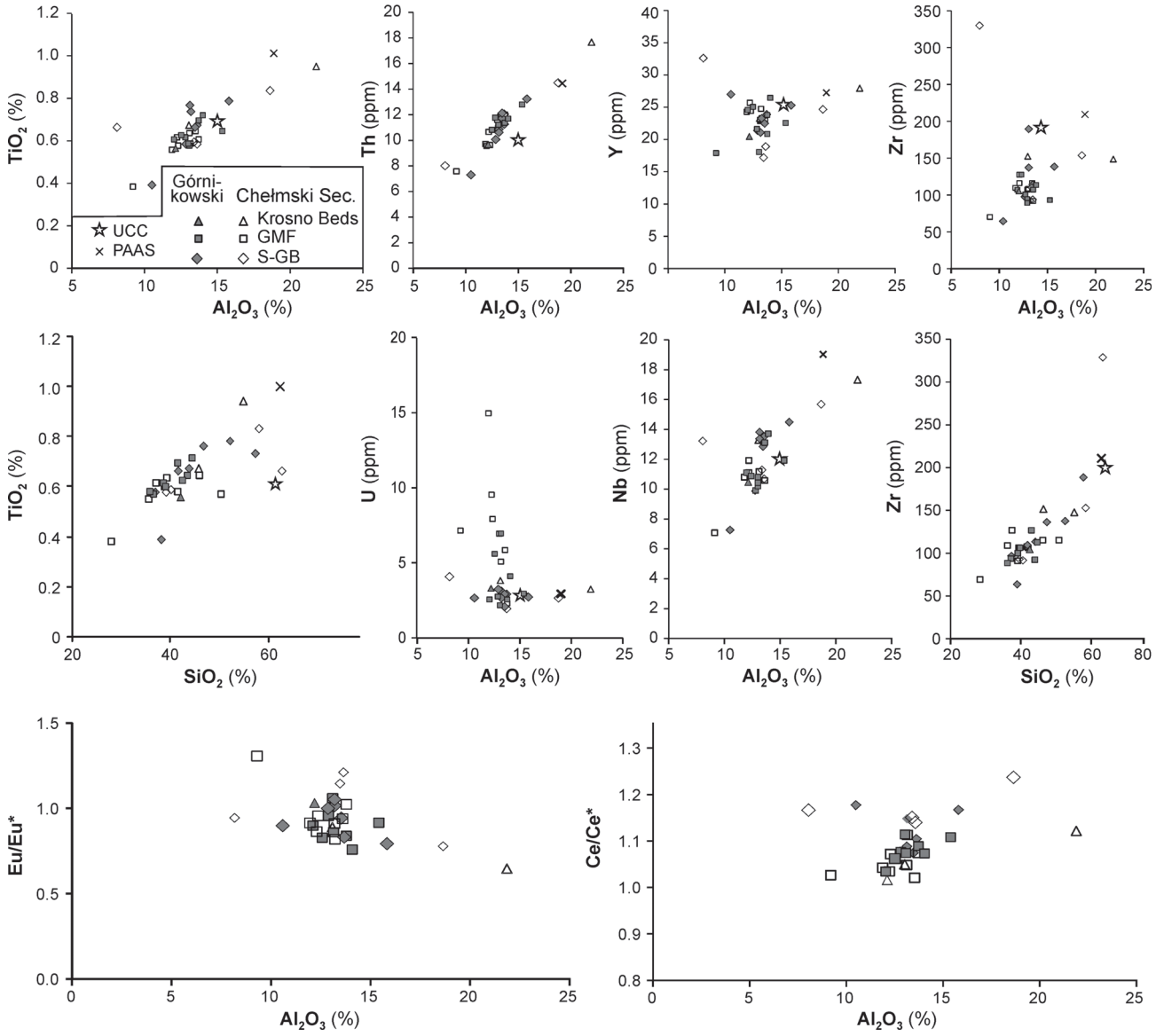

Fig. 7. Interactions between selected major and trace elements in the Sub-Grybów Beds, Grybów Marl Formation and Krosno Beds of the Grybów Nappe from the Ropa tectonic window.

rock with chemical composition similar to granite. The CIA values varying from 72.4 to 80.6 correlate with CPA that are between 90.5 and 96.5. Both CIA and CPA indicate intense weathering of the source rocks.

Sedimentary processes cause fractionation of stable weathering quartz and heavy minerals from clay minerals. Th and Nb correlate with TiO_2 and Al_2O_3 suggesting affinity of Th, Nb and TiO_2 to phyllosilicates. Positive correlation between TiO_2, Zr, Y and SiO_2 may imply presence of rutile and zircon sorted together with quartz (see Fig. 7). Ternary diagram plotting $10\times Al_2O_3$–Zr–$200\times TiO_2$ (Fig. 10) illustrates the presence of sorting-related fractionations (Garcia et al. 1991). Zircon is a carrier mineral for Zr and HREE plus Y, thus HREE and Y often co-vary with Zr. Accumulation of TE and SiO_2 co-occurs sometimes with Al_2O_3 (e.g. 24/05/N and 34/05/N) suggesting that material is worse sorted.

The Zr/Sc ratio is a useful index of sediment recycling (Hassan et al. 1999). When Zr/Sc is plotted against Th/Sc (McLennan et al. 1993), Zr enrichment during sorting can be evaluated. In the Zr/Sc vs. Th/Sc diagram (Fig. 11) samples fall along a trend involving zircon addition suggestive of a recycling effect.

Petrographic and geochemical indices of redeposition

An abundant matrix enclosing lithic particles within the S-GB, GMF and Krosno Beds determines their peculiar geochemical greywacke character. Occurrences of rounded grains of heavy minerals and stable for weathering inert macerals (inertinite) indicate enhanced contribution of recycled material within the Grybów Nappe sediments. More pelagic marls of the GMF contain smaller amounts of detritus.

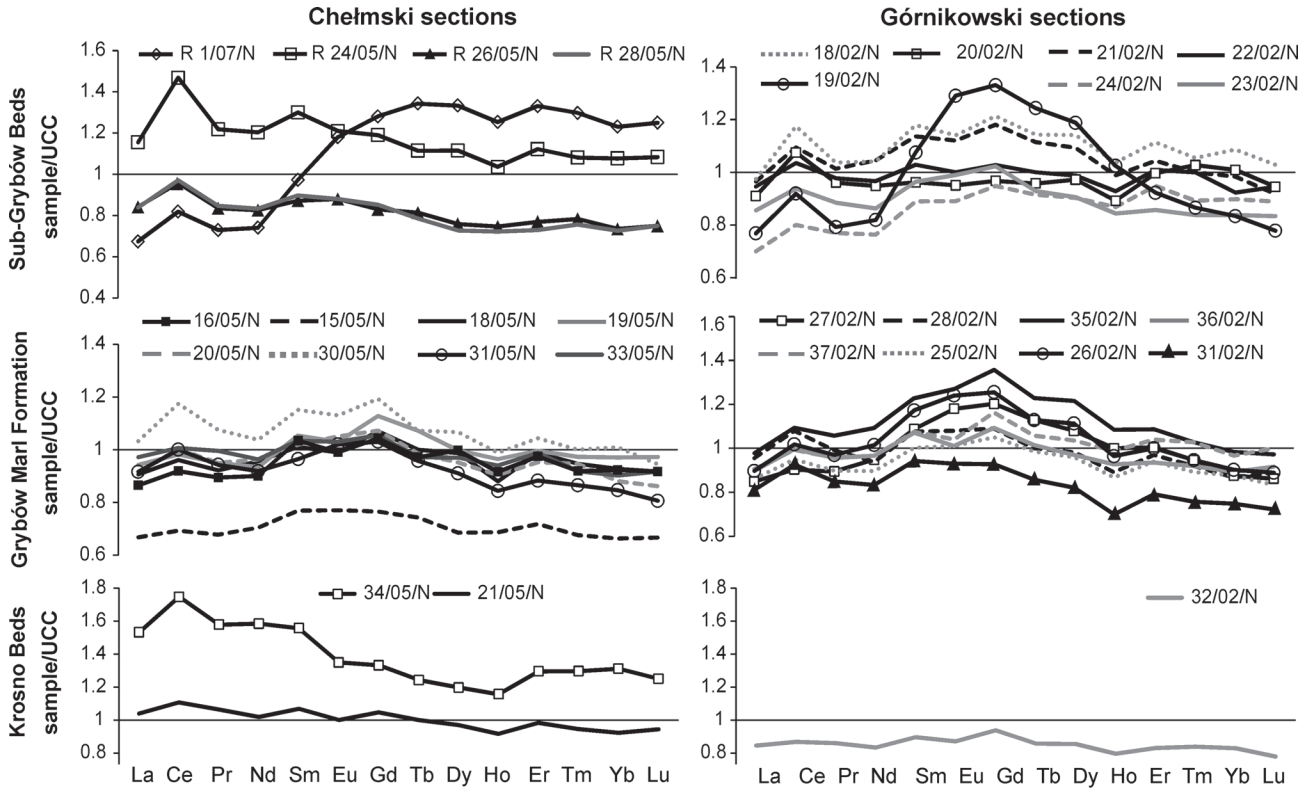

Fig. 8. Upper Continental Crust (UCC) — normalized REE patterns of the Sub-Grybów Beds, Grybów Marl Formation and Krosno Beds of the Grybów Nappe from the Ropa tectonic window. UCC data from Rudnick & Gao (2003) and Hu & Gao (2008), Post-Archean Australian Shale (PAAS — Taylor & McLennan 1985).

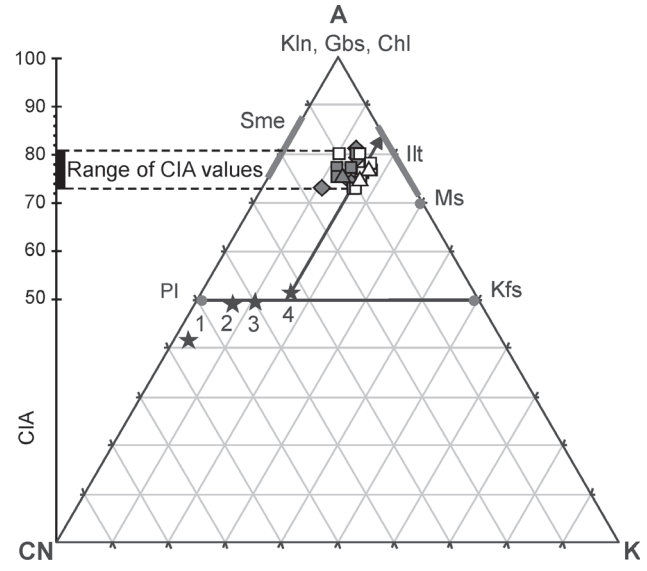

Fig. 9. A–CN–K diagram. **A** — Al_2O_3, **CN** — CaO^*+Na_2O, **K** — K_2O, in molecular proportions (Nesbitt & Young 1984) for the Sub-Grybów Beds, Grybów Marl Formation and Krosno Beds of the Grybów Nappe from the Ropa tectonic window. **CIA** — Chemical Index of Alteration (Nesbitt & Young 1982), **Chl** — chlorite, **Gbs** — gibbsite, **Ilt** — illite, **Kfs** — K-feldspar, **Kln** — kaolinite, **Ms** — muscovite, **Pl** — plagioclase, **Sme** — smectite. **1** — gabbro, **2** — tonalite, **3** — granodiorite, **4** — granite typical igneous rock averages from Fedo et al. (1997). Solid arrow indicates the theoretical weathering trend for granite.

In a diagram of $\lg(SiO_2/Al_2O_3)$ vs. $\lg(Fe_2O_3/K_2O)$, proposed by Herron (1988) to classify the terrigenous sands and shales, the samples are within the fields of shale and greywacke (Fig. 12). Due to higher contents of Fe_2O_3 two samples of the S-GB (19/02/N, 1/07/N) are classified as Fe-shale and Fe-sandstone respectively. Chemical composi-

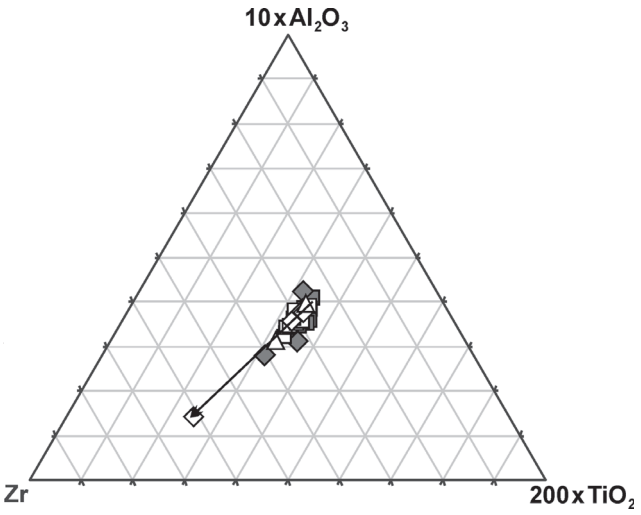

Fig. 10. Ternary $10\times Al_2O_3$–$200\times TiO_2$–Zr plot (after Garcia et al. 1994) showing possible sorting trend for the Sub-Grybów Beds, Grybów Marl Formation and Krosno Beds of the Grybów Nappe from the Ropa tectonic window. For explanation see Fig. 7.

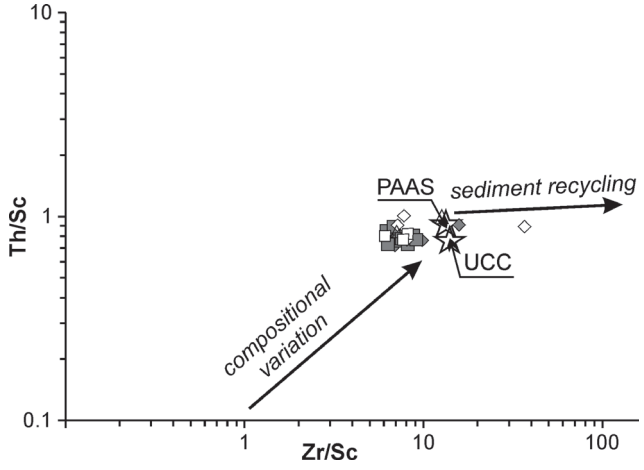

Fig. 11. Th/Sc vs. Zr/Sc provenance and recycling discrimination plot (after McLennan et al. 1990) for the Sub-Grybów Beds, Grybów Marl Formation and Krosno Beds of the Grybów Nappe from the Ropa tectonic window. For explanation see Fig. 7.

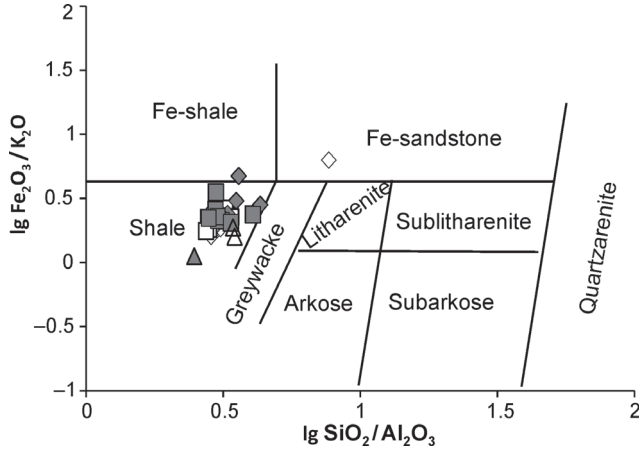

Fig. 12. Lg(Fe_2O_3/K_2O) vs. lg(SiO_2/Al_2O_3) diagram after Herron (1988) for the Sub-Grybów Beds, Grybów Marl Formation and Krosno Beds of the Grybów Nappe from the Ropa tectonic window. For explanation see Fig. 7.

tion is inferred from the presence of glauconite, Fe-oxyhydroxides and Fe-Mg carbonates, which are confirmed by microscopic and XRD analysis (see Figs. 5, 6). Glauconite is a frequent mineral in the S-GB and GMF. Detritus accumulated in sediments of the S-GB and GMF could be transported from the shelf, where glauconite was formed.

Depositional redox conditions and the influence of diagenetic processes

Negative correlation between Eu/Eu* and Al_2O_3 supports the authigenic origin of Eu anomaly, which generally reflects alteration of Eh conditions in the deposit (Elderfield & Sholkovitz 1987). Negative Eu anomaly suggests reductive conditions when the GMF was formed (e.g. 19/05/N, 30/05/N and 37/02/N; MacRae et al. 1992). The reductive conditions also exert influence on the U contents (Jones & Manning 1994) that are enhanced in the black samples of the GMF (15/05/N, 19/05/N, 20/05/N). The concentration of U reveals no correlation with Al_2O_3 (see Fig. 7) supporting its non-terrigenous derivation.

The Ce anomalies are more positive in the S-GB and decrease to mildly above unity in the GMF and Krosno Beds. If a positive-trending cerium anomaly had indicated oxic conditions and/or a sea-level fall (Elderfield & Sholkovitz 1987), decreasing of oxide availability and/or sea-level rise and influences of precipitation of marine carbonates could have governed during deposition of the GMF. On the other hand, positive correlation of Ce/Ce* to Al_2O_3 in the S-GB and Krosno Beds indicates rather a detrital contribution of the Ce anomaly.

The distribution patterns of REE of material studied usually differ from those of PAAS and UCC, because the REE distribution of fine-grained deposits is chiefly influenced by depositional and subsequent processes (Murray et al. 1990, 1992). Distributions of REE vary considerably as a function of uptake of REE by organic and/or oxyhydroxide grain coatings (Palmer 1985; Grandjean-Lécuyer et al. 1993; Sholkovitz et al. 1994) and variations in redox conditions (e.g. Elderfield et al. 1990). MREE-enrichment in phosphate (Byrne et al. 1996) can be a result of selective REE scavenging by algae (Stanley & Byrne 1990) or bacteria (Cruse et al. 2000). The strongly convex pattern at MREE suggests either enrichment in MREE or relative depletion in adjacent REE during deposition and/or diagenesis. MREE enrichment can by related to reductive conditions in the black shales (19/05/N, 30/05/N, 37/02/N) or to diagenetic Fe-Mn-Mg mineralization (18/02/N, 19/02/N, 35/02/N, 33/05/N). Phosphate is probably a carrier phase of MREE in the samples 27/02/N, 35/02/N, 16/05/N, 20/05/N, of which 16/05/N, 20/05/N are brown marly shales, therefore organic influence may also be considered for them.

Discussion

The position and age of the youngest deposits, beneath the Magura Nappe sole thrust, determine both the minimal amplitude of the Magura Nappe overthrust as well as the time in which the overthrusting of this unit begun. The youngest deposits from the Ropa tectonic window belong to the Late Oligocene — NP24 and NP25 zones and record the termination of Fore-Magura basins.

Reworked microfossils correlated with mineral and chemical composition can provide information on the processes of source rock erosion, transportation, sedimentation and preservation.

The allochthonous nannoflora consists of Cretaceous, Early, Middle Eocene and Late Eocene-Early Oligocene taxa. Various age distributions provide an insight into the Cretaceous to Cenozoic sediment reworking history in the remnant flysch basin (see also Švábenická et al. 2007; Oszczypko-Clowes 2012). Cretaceous species, as well as Early Eocene taxa, are reworked into Middle Eocene sediments. These sediments, probable formed low, consolidated basin slopes periodically incorporated into gravity flows.

The presence of reworked Oligocene nannofossils shows a more or less continuous erosion of newly deposited sediments on the sea floor during the Late Oligocene.

The contribution of recycled material within the Grybów Nappe sediments is inferred from occurrences of inertinite and rounded grains of glauconite and heavy minerals. In the Zr/Sc vs. Th/Sc diagram (Fig. 11) samples fall along a trend involving zircon addition suggestive of a recycling effect. The percentage of reworked species and visible discrepancy between sections can be clearly associated with lithology as well as with the distance from the source area. The Górnikowski sections are characterized by higher content of clastic material. The samples from the Chełmski sections contain more clay fraction than the Górnikowski section samples, as is shown in the diagram of $lg(SiO_2/Al_2O_3)$ vs. $lg(Fe_2O_3/K_2O)$ (Fig. 12) and by higher CIA and CPA values. Positive correlation between TiO_2, Zr, Y and SiO_2 (see Fig. 7), suggesting presence of rutile and zircon sorted together with quartz is mostly evident for the Chełmski section samples. It is confirmed by the ternary diagram $10\times Al_2O_3$–Zr–$200\times TiO_2$ (Fig. 10) illustrating the sorting-related fractionations (Garcia et al. 1991). The Chełmski sections display more distal facies of turbidites. The GMF collected from here are enriched in U and MREE (Table 4, Figs. 7, 8) that can be read as indicators of anoxic and reductive conditions during deposition and early diagenesis. Bottom water was hardly disturbed and freshened by declining turbidity currents.

The lack of Paleocene and Early Eocene nannofloral elements is probably due to the unavailability of sediments of these ages for reworking processes. The diversity of Paleocene and Early Eocene index species and their resistance to degradation would permit them to be abundant in Cenozoic flysch sediments. The same reworking pattern was observed throughout the entire flysch belt of the Outer Dinaride nappe front by Mikes et al. (2008).

During the Late Eocene–Oligocene, as results of regional compression in the Alpine area, prominent paleogeographic changes took place in the Outer Carpathian sedimentary area, which was transformed from remnant oceanic basin into a flexural foreland basin (Oszczypko 1999). It was manifested by shallowing of all sub-basins and isolation from oceanic areas (Van Couvering et al. 1981; Oszczypko-Clowes 2001). The deposition of deep-water basinal turbidites was substituted by pelagic Submenilite *Globigerina* Marls (SGM). Finally during the Rupelian this resulted in decline of the circulation of currents, followed by the reduced oxygen environment, with eutrophic population of microfossils, and deposition, under anoxic bottom water conditions, of dark organic-rich shales of the Menilite formation (Bessereau et al. 1996; Pícha & Stráník 1999; Oszczypko-Clowes & Żydek 2012). At the same time the emerging Fore-Magura Ridge, which was the prolongation of the Marmarosh Massif (Oszczypko et al. 2005) separated the Dukla-Grybów sub-basin from the Magura Basin. The Oligocene Dukla succession become a part of the Silesian Basin that was supplied from the south (Unrug 1968), as is proved by the analyses of paleotransport directions indicating the transport of clastic material from the south-east and the south.

The Oligocene–Early Miocene closing of the northern sector of the Outer Carpathian sedimentary area is manifested by the deposition of the Krosno synorogenic lithofacies, which occupied the Grybów-Dukla-Silesian/Sub-Silesian/Skole and Boryslav-Pokuttya basin system.

During the latest Oligocene period the thrusting of the Magura Nappe onto the Fore-Magura (Dukla and Grybów) sedimentary area began to occur. From latest Oligocene to late Badenian (9–10 Ma; see Oszczypko 1998) the front of the Magura Nappe progressed towards the north. As a result the Grybów Unit, with reduced thickness, is wedged between the Magura Nappe and Dukla Unit. In surface exposures the Grybów Unit reveals thrust sheet structure.

The Ropa tectonic window developed during the Middle Miocene thrusting of the Magura Nappe against its foreland.

Conclusions

- The youngest deposits from the Ropa tectonic window belong to the Late Oligocene — NP24 and NP25;
- The Grybów Succession records the terminal stage of the Fore-Magura Basin development;
- These synorogenic turbidites facies are characterized by a medium level of reworked nanofossils;
- A high contribution of recycled material is inferred from presence of lithic grains, abraded heavy minerals (zircon and rutile), rounded glauconite as well as inert macerals (inertinite). Enrichment in zircon and rutile is confirmed geochemically by positive correlation between Zr, SiO_2 and TiO_2. It is also plotted on $10\times Al_2O_3$–Zr–$200\times TiO_2$ and Zr/Sc vs. Th/Sc diagrams. The source rocks are chemically similar to granites, that were affected by strong weathering shown in the A–CN–K diagram, and by high values of CIA and CPA;
- Chełmski sections display more distal facies of turbidites. The sediments consist of less detritus, which represents mainly clay fraction and is well-sorted. It corresponds to the lower frequency of reworked nanofossils;
- Brownish-black sediments of the GMF were formed under anoxic and reductive conditions;
- Post-depositional processes are recorded by Fe-Mn-Mg mineralization, phosphate precipitation, REE fractionation and U enrichment.

Acknowledgments: The authors wish to thank Katarína Šarinová and Diego Puglisi for their constructive criticism and detailed review of the manuscript. Ján Soták is also gratefully acknowledged for his valuable comments on the manuscript. The research was undertaken as part of a Project of the Polish Ministry of Science and Higher Education Grant (No. N N307 531038).

References

Aubry M.P. 1984: Handbook of Cenozoic calcareous nannoplankton. Book 1: Ortholithae (Discoasters). *Micropaleontology Press, Amer. Mus. Natur. Hist.*, New York, 1–265.

Aubry M.P. 1988: Handbook of Cenozoic calcareous nannoplankton. Book 2: Ortholithae (Holochoccoliths, Ceratoliths and others). *Micropaleontology Press*, *Amer. Mus. Natur. Hist.*, New York, 1–279.

Aubry M.P. 1989: Handbook of Cenozoic calcareous nannoplankton. Book 3: Ortholithae (Pentaliths, and others) Heliolithae (Fasciculiths, Sphenoliths and others). *Micropaleontology Press*, *Amer. Mus. Natur. Hist.*, New York, 1–279.

Aubry M.P. 1990: Handbook of Cenozoic calcareous nannoplankton. Book 4: Heliolithae (Helicoliths, Cribriliths, Lopadoliths and others). *Micropaleontology Press*, *Amer. Mus. Natur. Hist.*, New York, 1–381.

Aubry M.P. 1999: Handbook of Cenozoic calcareous nannoplankton. Book 5: Heliolithae (Zygolithus and Rhabdolithus). *Micropaleontology Press*, *Amer. Mus. Natur. Hist.*, New York, 1–367.

Bessereau G., Roure F., Kotarba M., Kusmirek J. & Strzetelski W. 1996: Structure and hydrocarbon habitat of the Polish Carpathians. In: Ziegler P.A. & Horváth F. (Eds.): Peri-Tethys Memoir 2: Structure and prospects of Alpine basins and forelands. *Mém. Mus. Nat. Hist. Natur.* 170, 343–373.

Biolzi M., Műller C. & Palmieri G. 1981: Calcareous nannoplankton. In: Gelati R. & Steininger F. (Eds.): In search of the Paleogene–Neogene boundary stratotype. Part II. *Riv. Ital. Paleont. Stratigr.* 89, 4, 460–471.

Bizon G. & Műller C. 1979: Remarks on the Oligocene/Miocene boundary based on the results obtained from the Pacific and the Indian Ocean. *Ann. Géol. Pays Hellén.* 1, 101–111.

Blaicher J. 1958: The microfauna of the Magura Series of the Grybów region (Middle Carpathians). *Geol. Quarterly* 2, 385–399 (in Polish with English summary).

Bown P.R. (Ed.) 1998: Calcareous Nannofossil biostratigraphy. *British Micropalaeont. Soc. Ser., Kluwer Academic Publishers*, Cambridge, 1–315.

Bukry D. 1973: Low-latitude coccolith biostratigraphic zonation. *Init. Repts. Deep Sea Drill. Proj.* 15, 127–149.

Burtan J., Cieszkowski M., Jawor E. & Ślączka A. 1992: Dąbrowa — Geology of the Klęczany-Limanowa tectonic window. [Dąbrowa-Budowa okno tektonicznego Klęczan-Limanowej.] In: Zuchiewicz W. & Oszczypko N. (Eds.): A guidebook of 63th Annual Meeting of Polish Geological Society, Koninki, 17–19 September 1992. *Jagiellonian Univ., Inst. Geol. Sci.*, Kraków, 171—179 (in Polish).

Byrne R.H., Liu X. & Schijf J. 1996: The influence of phosphate coprecipitation on rare earth distribution in natural waters. *Geochim. Cosmochim. Acta* 60, 3341–3346.

Cieszkowski M. 1992: Michalczowa zone: a new unit of the fore-Magura zone, Outer West Carpathians, South Poland. [Strefa Michalczowej — nowa jednostka strefy przedmagurskiej w zachodnich Karpatach fliszowych i jej geologiczne znaczenie.] *Zesz. Nauk. AGH, Geologia* 18, 1–2, 1–125 (in Polish).

Cruse A.M., Lyons T.W. & Kidder D.L. 2000: Rare-earth element behavior in phosphates and organic-rich host shales: an example from the Upper Carboniferous of midcontinent North America. In: Glenn C.R., Prévot L. & Lucas J. (Eds.): Marine authigenesis: from global to microbial. *SEPM Spec. Publ.* 66, 445–453.

Cullers R.L. 2000: The geochemistry of shales, siltstones and sandstones of Pennsylvanian–Permian age, Colorado, USA: implications for provenance and metamorphic studies. *Lithos* 51, 181–203.

de Kaenel E. & Villa G. 1996: Oligocene–Miocene calcareous nannofossil biostratigraphy and paleoecology from the Iberia Abyssal Plain. *Proc. ODP, Sci. Results* 149, 79–145.

Elderfield H. & Sholkovitz E.R. 1987: Rare earth elements in the pore waters of reducing nearshore sediments. *Earth Planet. Sci. Lett.* 82, 280–288.

Elderfield H., Upstill-Goddard R. & Sholkovitz E.R. 1990: The rare earth elements in rivers, estuaries, and coastal seas and their significance to the composition of ocean waters. *Geochim. Cosmochim. Acta* 54, 971–991.

Fedo C.M., Young G.M. & Nesbitt G.M. 1997: Paleoclimatic control on the composition of the Paleoproterozoic Serpent Formation, Huronian Supergroup, Canada: A greenhouse to icehouse transition. *Precambrian Res.* 86, 201–223.

Garcia D., Coelho J. & Perrin M. 1991: Fractionation between TiO_2 and Zr as a measure of sorting within shale and sandstone series (Northern Portugal). *Eur. J. Mineral.* 3, 401–414.

Garcia D., Fonteilles M. & Moutte J. 1994: Sedimentary fractionations between Al, Ti and Zr and the genesis of strongly peraluminous granites. *J. Geology* 102, 411–422.

Gedl P. 2005: Stop 1 — Ropa: palaeoenvironmental changes across the Eocene–Oligocene boundary in the Flysch Carpatian basins. In: Excursion guide of 5th Micropaleontological Workshop, Szymbark, Poland, June 8–10, 2005. *Instytut Nauk Geologicznych PAN*, Kraków, 65–68.

Grandjean-Lécuyer P., Feist R. & Albarède F. 1993: Rare earth elements in old biogenic apatites. *Geochim. Cosmochim. Acta* 57, 2507–2514.

Hassan S., Ishiga H., Roser B.P., Dozen K. & Naka T. 1999: Geochemistry of Permian Triassic shales in the Salt range, Pakistan: implications for provenance and tectonism at the Gondwana margin. *Chem. Geol.* 168, 293–314.

Herron M.M. 1988: Geochemical classification of terrigenous sands and shales from core or log data. *J. Sed. Petrology* 58, 820–829.

Hofer G., Wagreich M. & Neuhuber S. 2013: Geochemistry of fine-grained sediments of the upper Cretaceous to Paleogene Gosau Group (Austria, Slovakia): Implications for paleoenvironmental and provenance studies. *Geosci. Frontiers* 4, 449–468.

Hu Z. & Gao S. 2008: Upper crustal abundances of trace elements: A revision and update. *Chem. Geol.* 253, 205–221.

Jones B. & Manning D.A.C. 1994: Comparison of geochemical indices used for the interpretation of paleoredox conditions in ancient mudstones. *Chem. Geol.* 111, 111–129.

Koráb T. & Ďurkovič T. 1978: Geology of Dukla Unit (East-Slovakian Flysch). *Geologický Ústav Dionýza Štúra*, Bratislava, 1–196 (in Slovak with English summary).

Kováč M., Plašienka D., Soták J., Vojtko R., Oszczypko N., Less G. & Králiková S. (in print): Western Carpathians Palaeogene paleogeography and basin development: a case study within the scope of the ALCAPA terrane.

Kozikowski H. 1956: Ropa-Pisarzowa unit, a new tectonic unit of the Polish flysch Carpathians. *Biul. Inst. Geol.* 110, 93–137 (in Polish with English summary).

Kozikowski H. & Jednorowska A. 1957: The problem of the age of the Grybow Beds and so called "Gray chalk" in the vicinity of Gorlice. [Problem wieku warstw grybowskich i tzw. "szarej kredy" z okolic Gorlic.] *Przegl. Geol.* 5, 3, 100–137 (in Polish with English summary).

Książkiewicz M. 1972: Geology of Poland, v. IV Tectonics, part 3 Carpathians. [Budowa geologiczna Polski , t. IV Tektonika, cz. 3 Karpaty.] *Wyd. Geol.*, Warszawa, 1–228 (in Polish).

Leszczyński S. 1997: Origin of the Sub-Menilite Globigerina Marl (Eocene–Oligocene transition) in the Polish Outer Carpathians. *Ann. Soc. Geol. Pol.* 67, 367–427.

MacRae N.D., Nesbitt H.W. & Kronberg B.I. 1992: Development of a positive Eu anomaly during diagenesis. *Earth Planet. Sci. Lett.* 109, 585–591.

Maiorano P. & Monechi S. 2006: Early to Late Oligocene calcareous nannofossil bioevents in the Mediterranean (Umbria-Marche basin, central Italy). *Riv. Ital. Paleont. Stratigr.* 12, 261–273.

Martini E. 1971: Standard Tertiary and Quaternary calcareous nannoplankton zonation. In: Farinacci A. (Ed.): Proc. II. Planktonic Conf. Roma 1970, Vol. 2. *Edizioni Tecnoscienza*, Rome, 729–785, pls. 1–4.

Martini E. & Müller C. 1986: Current Tertiary and Quaternary calcareous nannoplankton stratigraphy and correlations. *Newslett.*

Stratigr. 16, 2, 99–112.

McLennan S.M., Hemming D.K. & Hanson G.N. 1993: Geochemical approaches to sedimentation, provenance, and tectonics. *Geol. Soc. Amer., Spec. Publ.* 284, 21–40.

McLennan S., Taylor S., McCulloch M. & Maynard J. 1990: Geochemical and Nd-Sr isotopic composition of deep-sea turbidites: Crustal evolution and plate tectonic associations. *Geochim. Cosmochim. Acta* 54, 2015–2050.

Melinte M. 1995: Changes in nannofossil assemblages during the Oligocene–Lower Miocene interval in the Eastern Carpathians and Transylvania. In: Abstracts 10th RCMNS, Bucharest 1995. *Rom. J. Stratigraphy* 76, suppl. 7, 171–172.

Melinte M. 2005: Oligocene palaeoenvironmental changes in the Romanian Carpathians, revealed by calcareous nannofossils. In: Tyszka J., Oliwkiewicz-Miklasinska M., Gedl P. & Kaminski M. (Eds.): Methods and applications in micropalaeontology. *Stud. Geol. Pol.* 124, 341–352.

Melinte-Dobrinescu M. & Brustur T. 2008: Oligocene–Lower Miocene events in Romania. *Acta Palaeont. Rom.* 6, 203–215.

Mikes T., Báldi-Béke M., Kazmer M., Dunkl I. & von Eynatten H. 2008: Calcareous nannofossil age constraints on Miocene flysch sedimentation in the Outer Dinarides (Slovenia, Croatia, Bosnia-Herzegovina and Montenegro). In: Siegesmund S., Fugenschuh B. & Froitzheim N. (Eds.): Tectonic aspects of the Alpine-Dinaride-Carpathian system. *Geol. Soc. London, Spec. Publ.* 298, 335–363.

Murray R.W., Buchholtz Tenbrink M.R., Jones D.L., Gerlach D.C. & Russ G.P. III 1990: Rare earth elements as indicators of different marine depositional environments in chert and shale. *Geology* 18, 268–271.

Murray R.W., Buchholtz Tenbrink M.R., Gerlach D.C., Russ G.P. III & Jones D.L. 1992: Interoceanic variation in the rare earth, major, and trace element depositional chemistry of chert: Perspectives gained from the DSDP and ODP record. *Geochim. Cosmochim. Acta* 56, 1897–1913.

Nesbitt H.W. & Young G.M. 1982: Early Proterozoic climates and plate motions inferred from major element chemistry of lutites. *Nature* 199, 715–717.

Nesbitt H.W. & Young G.M. 1984: Prediction of some weathering trends of plutonic and volcanic rocks based on thermodynamic and kinetic considerations. *Geochim. Cosmochim. Acta* 48, 1523–1534.

Olszewska B. 1981: On same assemblages of small foraminifers of the windows series of Sopotnia Mała, Mszana Dolna, Szczawa and Klęczany. *Biul. Inst. Geol.* 331, 141–163 (in Polish with English summary).

Olszewska B. 1983: A contribution of the knowledge of planktonic foraminifers of the Globigerina Submenilite Marls of the Polish Outer Carpathians. *Kwart. Geol.* 27, 546–570 (in Polish).

Oszczypko (Clowes) M. 1996: Calcareous nannoplankton of the Globigerina Marls (Leluchów Marls Member), Magura Nappe, West Carpathians. *Ann. Soc. Geol. Pol.* 66, 1–15.

Oszczypko N. 1998: The Western Carpathian Foredeep — development of the foreland basin in front of the accretionary wedge and its burial history (Poland). *Geol. Carpathica* 49, 6, 415–431.

Oszczypko N. 1999: From remnant oceanic basin to collision-related foreland basin — a tentative history of the Outer Western Carpathians. *Geol. Carpathica*, *Spec. Issue* 50, 161–163.

Oszczypko N. & Oszczypko-Clowes M. 2011: Stratigraphy and tectonics of the Świątkowa Wielka Tectonic Window (Magura Nappe, Polis Outer Carpathians). *Geol. Carpathica* 62, 139–154.

Oszczypko N., Ślączka A. & Żytko K. 2008: Tectonic subdivision of Poland: Polish Outer Carpathians and their fore-deep. *Przegl. Geol.* 10, 927–935 (in Polish with English summary).

Oszczypko N., Oszczypko-Clowes M., Golonka J. & Krobicki M. 2005: Position of the Marmarosh Flysch (Eastern Carpathians) and its relation to the Magura Nappe (Western Carpathians). *Acta Geol. Hung.* 48, 3, 259–282.

Oszczypko-Clowes M. 2001: The nannofossil biostratigraphy of the youngest deposits of the Magura Nappe (East of the Skawa river, Polish Flysch Carpathians) and their palaeoenvironmental conditions. *Ann. Soc. Geol. Pol.* 71, 139–188.

Oszczypko-Clowes M. 2008: The stratigraphy of the Oligocene deposits from the Ropa tectonic window (Grybów Nappe, Western Carpathians, Poland). *Geol. Quarterly* 52, 127–142.

Oszczypko-Clowes M. 2012: Reworked nannofossils from the youngest flysch deposits in the Magura Nappe (Outer Western Carpathians, Poland) — A case study. *Geol. Carpathica* 63, 407–421.

Oszczypko-Clowes M. & Oszczypko N. 2004: The position and age of the youngest deposits in the Mszana Dolna and Szczawa tectonic windows (Magura Nappe, Western Carpathians, Poland). *Acta Geol. Pol.* 54, 339–367.

Oszczypko-Clowes M. & Ślączka A. 2006: Nannofossil biostratigraphy of the Oligocene deposits in the Grybów tectonic window (Grybów Unit, Western Carpathians, Poland). *Geol. Carpathica* 57, 473–482.

Oszczypko-Clowes M. & Żydek B. 2012: Paleoecology of the Late Eocene Early Oligocene Malcov Basin based on the calcareous nannofossils — a case study of the Leluchów section (Krynica Zone, Magura Nappe, Polish Outer Carpathians). *Geol. Carpathica* 63, 2,149–164.

Palmer M.R. 1985: Rare earth elements in foraminifera tests. *Earth Planet. Sci. Lett.* 73, 85–298.

Perch-Nielsen K. 1985: Cenozoic calcareous nannofossils. In: Bolli H., Saunders J.S. & Perch-Nielsen K. (Eds.): Plankton stratigraphy. *Cambridge University Press*, 11, 427–554.

Pícha F. & Stráník Z. 1999: Late Cretaceous to early Miocene deposits of the Carpathian foreland basin in southern Moravia. *Int. J. Earth Sci.* 88, 475–495.

Rudnick R.L. & Gao S. 2003: The composition of the continental crust. In: Holland H.D. & Turekian K.K. (Eds.): Treatise on geochemistry, the crust. *Elsevier-Pergamon*, 1–64.

Sholkovitz E.R., Landing W.M. & Lewis B.L. 1994: Ocean particle chemistry: The fractionation of rare earth elements between suspended particles and seawater. *Geochim. Cosmochim. Acta* 58, 1567–1579.

Sikora W. 1960: On the stratigraphy of the series in the tectonic window at Ropa near Gorlice (Western Carpathians). *Kwart. Geol.* 4, 152–170 (in Polish with English summary).

Sikora W. 1970: Geology of the Magura Nappe between Szymark Ruski and Nawojowa. *Biul. Inst. Geol.* 235, 5–121.

Stanley J.K., Jr. & Byrne R.H. 1990: The influence of solution chemistry on REE uptake by *Ulva lactuca* L. in seawater. *Geochim. Cosmochim. Acta* 54, 1587–1595.

Ślączka A. 1971: Geology of the Dukla Unit. *Prace Inst. Geol.* 1, 1–63 (in Polish with English summary).

Ślączka A. 1973: Field trip 1 — Grybów, Polany, Berest, Krzyżówka. [Wycieczka 1 — Grybów, Polany, Berest, Krzyżówka.] In: Żytko K. (Ed.): A geological guidebook to the Eastern Flysch Carpathians. *Wyd. Geol.,* 78–87 (in Polish).

Ślączka A. (Ed.) 1976: Atlas of paleotransport of detrital sediments in the Carpathian-Balkan Mountain System. *Inst. Geol.*, Warszawa.

Ślączka A., Kruglow S., Golonka J., Oszczypko N. & Popadyuk I. 2006: The general geology of the Outer Carpathians, Poland, Slovakia and Ukraine. In: Golonka J. & Picha F. (Eds.): The Carpathians and their foreland: Geology and hydrocarbon resources. *Amer. Assoc. Petrol. Geol. Mem.* 84, 221–258.

Ślączka A., Renda P., Cieszkowski M., Golonka J. & Nigro F. 2012: Sedimentary basin evolution and olistolith formation:

The case of Carpathian and Sicilian region. *Tectonophysics* 568–569, 306–319.

Śliwińska K., Abrahamsen N., Beyer C., Brünings-Hansen T., Thomsen E., Ulleberg K. & Heilmann-Clausen C. 2012: Bio- and magnetostratigraphy of Rupelian–mid Chattian deposits from the Danish land area. *Rev. Palaeobot. Palynol.* 172, 48–69.

Świdziński H. 1963: Les couches de Grybów et leur importance pour latectonique des Karpates. Resume des communications. *Congr. Geol. Assoc. Karpat.-Balk.,* Warszawa–Kraków, 6, 191–193.

Švábenická L., Bubík M. & Stráník Z. 2007: Biostratigraphy and paleoenvironmental changes on the transition from the Menilite to Krosno lithofacies (Western Carpathians, Czech Republic). *Geol. Carpathica* 58, 237–262.

Taylor S.R. & McLennan S.M. 1985: The continental crust: Its composition and evolution. *Blackwell Scientific*, Oxford, 1–312.

Uhlig V. 1888: Ergebnisse geologischer Aufnahmen in den westgalizischen Karpathen. *Jb. Geol. Reichsanstalt* 38, 85–264.

Unrug R. 1968: Silesia Ridge as a source area for clasticmaterial in flysch sandstone of Beskid Śląski and Wyspowy (Polish Western Carpathians). [Kordyliera śląska jako obszar źródłowy materiału klastycznego piaskowców fliszowych Beskidu Śląskiego i Beskidu Wysokiego (polskie Karpaty zachodnie).] *Rocz. Pol. Tow. Geol.* 38, 1, 81–164.

Van Couvering I.A., Aubry M.P., Berggren Q.A., Bujak J.P., Naesen C.W. & Wieser T. 1981: Terminal Eocene event and the Polish connections. *Palaeogeogr. Palaeoclimatol. Palaeoecol.* 36, 321–362.

Veizer J. & Mackenzie F.T. 2003: Evolution of sedimentary rocks. In: Holland H.D. & Turekian K.K (Eds): Treatise on geochemistry. Sediments, diagenesis and sedimentary rocks. *Elsevier,* Pergamon, 369–4077.

Wedepohl K.H. 1991: Chemical composition and fractionation of the continental crust. *Geol. Rdsch.* 80, 2, 207–223.

Whitney D.L. & Evans B.W. 2010: Abbreviations for names of rock-forming minerals. *Amer. Mineralogist* 95, 185–187.

Wójcik-Tabol P. & Ślączka A. 2013: Provenance of Lower Cretaceous deposits of the western part of the Silesian Nappe in Poland (Outer Carpathians): evidence from geochemistry. *Ann. Soc. Geol. Pol.* 83, 113–132.